

# The Complete Disturbance

How Does it All Fit Together



Janet Kozyra (University of Michigan)

# The Sun & Earth form a complex system with many interacting components that are themselves complex systems



Our ability to predict future states of this system have a direct benefit to a society increasingly reliant on technologies that are affected by the space environment (see D. Baker lecture).

Focus is on the interactions not the individual pieces.

The global system is dynamical and nonlinear.

There is a constant exchange of mass, energy and momentum across its open boundaries and between elements that drives it far from equilibrium.

Unlike systems in general , *complex* systems have the potential to produce unstable behaviors.

The Sun & Earth form a complex system which has characteristic properties

# Prediction is difficult based on knowledge of components alone

What we measure is actually the integrated response of the entire interconnected system which can be nonlinear and unstable.

- nonlinear: response is not the linear superposition of responses to individual processes

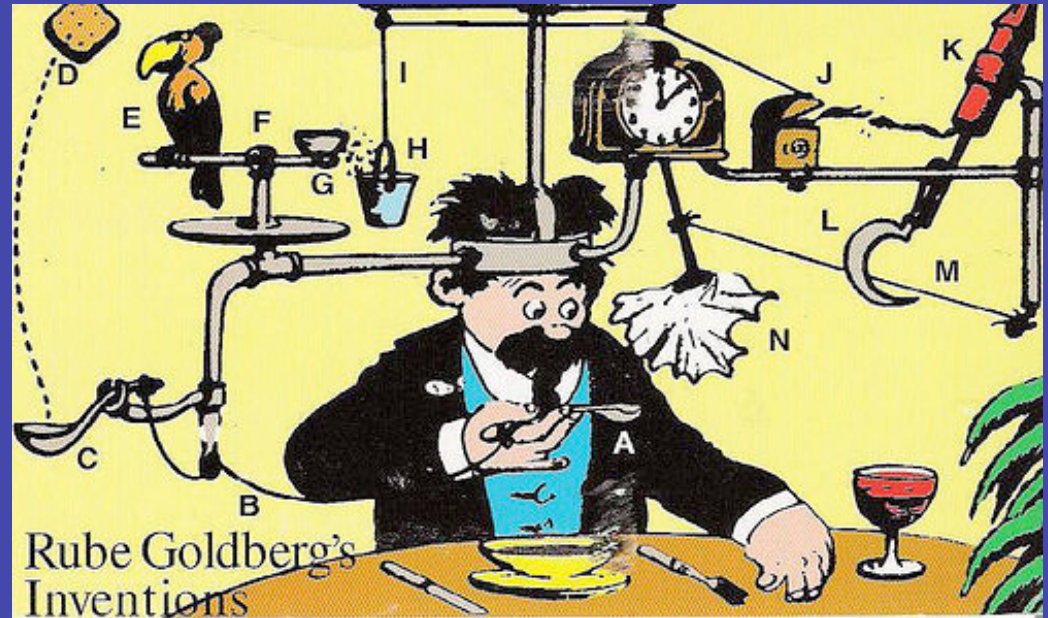


Disney's WALL-E (<http://adisney.go.com/disneyvideos/animatedfilms/wall-e/>)

“The whole is greater than the sum of the parts “

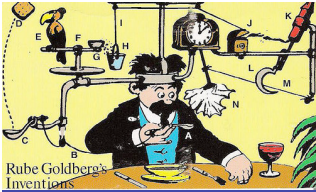
# Negative and Positive Feedbacks Develop

A particular disturbance can trigger multiple nonlinear feedbacks between system components, which can amplify, cancel out altogether, or even change the nature of the expected response.



[http://en.wikipedia.org/wiki/Rube\\_Goldberg\\_machine](http://en.wikipedia.org/wiki/Rube_Goldberg_machine)

“Simple cause & effect  
are rare.”



# Example

Solar Wind  
Electric Field



Increases polar cap  
potential drop ( $\Phi_{pc}$ )  
enhances convection

Reduces  
reconnection  
rate,  $\Phi_{pc}$ , &  
outflows

Greater  
centrifugal  
acceleration  
of upflows

Mass  
Loading of  
Convection

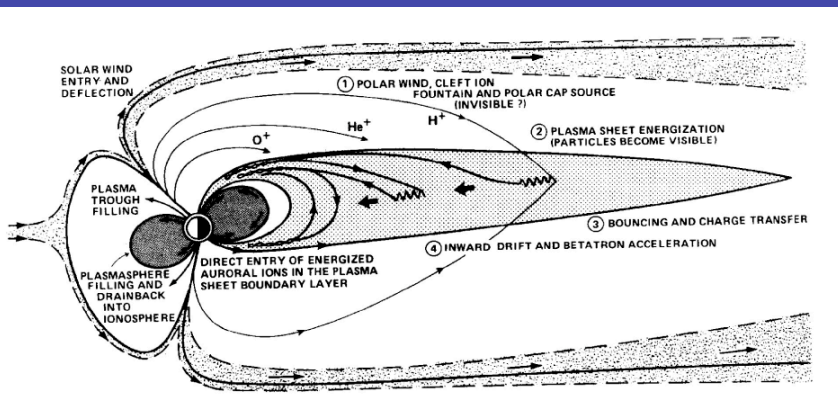
Mass-loading  
slows  
convection

More  
ionospheric  
outflow

Chappell et al., 1987

Higher  $O^+$   
content of  
plasmashet

Winglee et al., [2002], Lotko, [2007]



# History Matters

**Preconditioning** - a condition that must exist before something can occur

- Example: Northward IMF drives efficient capture of solar wind plasma triggering formation of superdense & cold plasma sheet material. If southward IMF closely follows, this material is delivered into the inner magnetosphere, acts as a source population for the ring current, and produces a more intense storm [c.f., *Thomsen et al.*, 2003].

## Memory

- Example: the neutral atmosphere is a key element in system memory. Lot of inertia and long time-scales. Preserves the history of recent energy inputs. Introduces solar cycle and seasonal effects.

**Initial Conditions** - Small changes in initial conditions can produce significant changes in system state



“Butterfly Effect”

# Emergent Features Appear

The source of phenomena can be contained in the interactions and not in the components themselves

No new components but unexpected features appear

One example of strong candidate for emergence:

- **Great Red Auroras**



Still from "The Mummy", Universal Pictures, 2008

“Science of Surprise”

# Emergence? Great Red Auroras



The great red aurora of 10-11 February 1958, the 13th largest magnetic storm in recorded history. Snow appeared red in Alaska and radio communications between the US and other parts of the world were disrupted. Photo credit: Bert Vorchheimer

Great red auroras occur *only* during extreme magnetic activity. Features [c.f. *Vallence-Jones*, 1992]:

- ❖ Red auroral displays of unusual brightness ( $> 100$  kR of 630 nm light)
- ❖ Extend to exceptionally low MLATs
- ❖ Cover up to 95% of the sky in places

Observations suggest these aurora are produced by 10-20 min bursts of large fluxes of soft electrons (10s to 100s eV) [c.f., *Robinson et al.*, 1985; *Shiokawa et al.*, 1997]. Source unknown.

For reasons not understood:

- ❖ Auroral precipitation softens in energy during intense storms [c.f., *Hecht et al.*, 2008]

# Summary: Complex System Properties

- ✓ Prediction is difficult based on knowledge of components alone
- ✓ Negative and Positive Feedbacks are Integral to System Behavior
- ✓ Small changes in initial conditions can affect the final state
- ✓ History Matters
- ✓ Emergent Features Appear

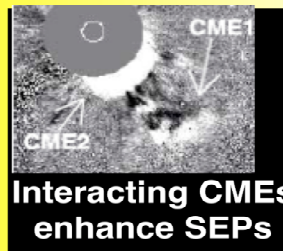
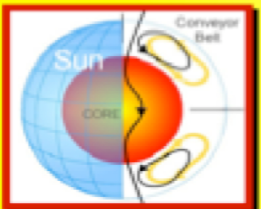
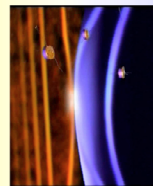
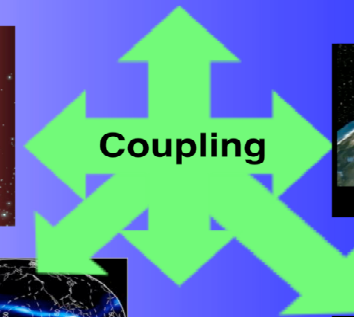
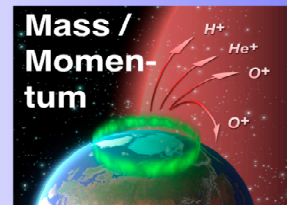
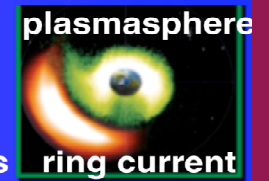
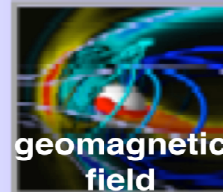
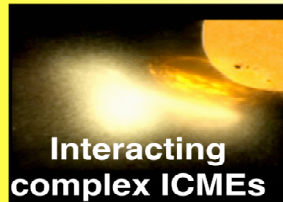
## Consequences:

- Interactions between components often define the system response Not contained in the individual pieces
- Clear cause and effect appears only when these effects are disentangled.
- For these cases, cannot break system into smaller digestible pieces for study

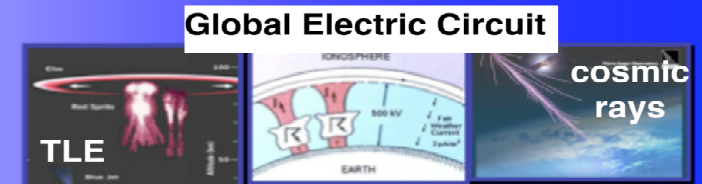
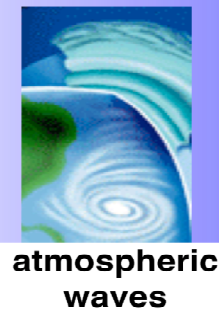
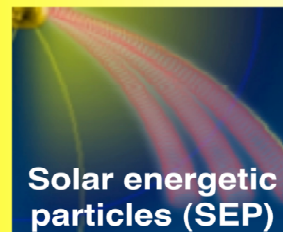
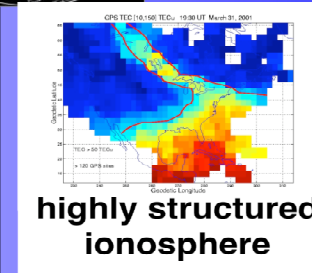
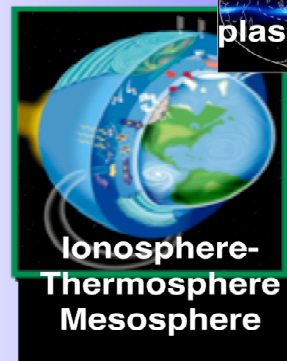
# Summary of interacting components?

Preconditioning Initial Conditions Memory Feedbacks Nonlinearity Instability Emergence

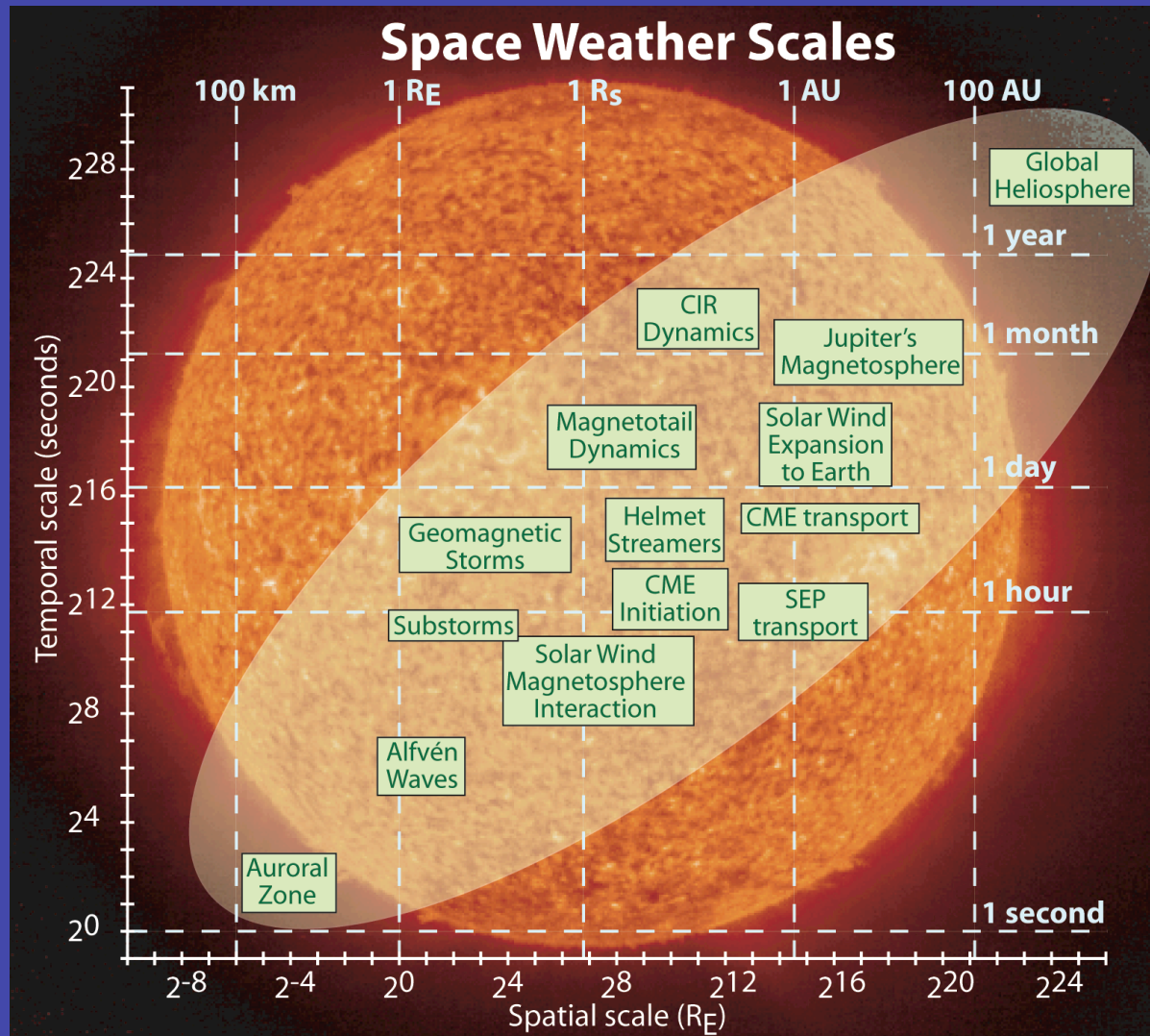
Cross-scale coupling



Solar wind energy input



# System is Multi-Scale & Couples between Scales



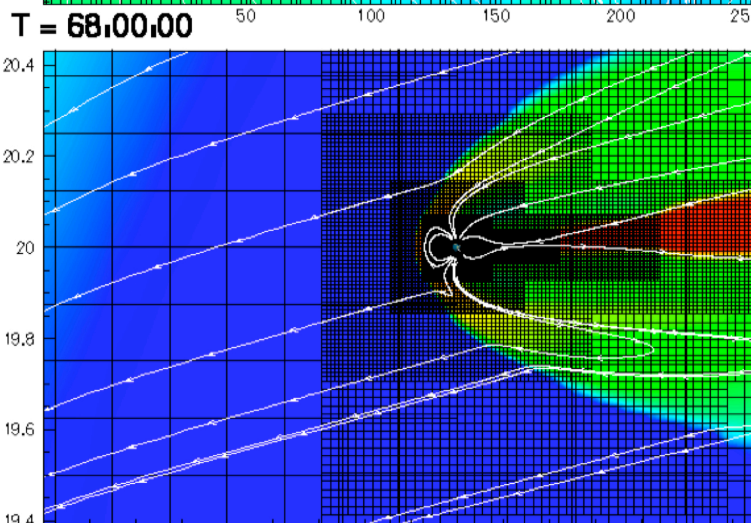
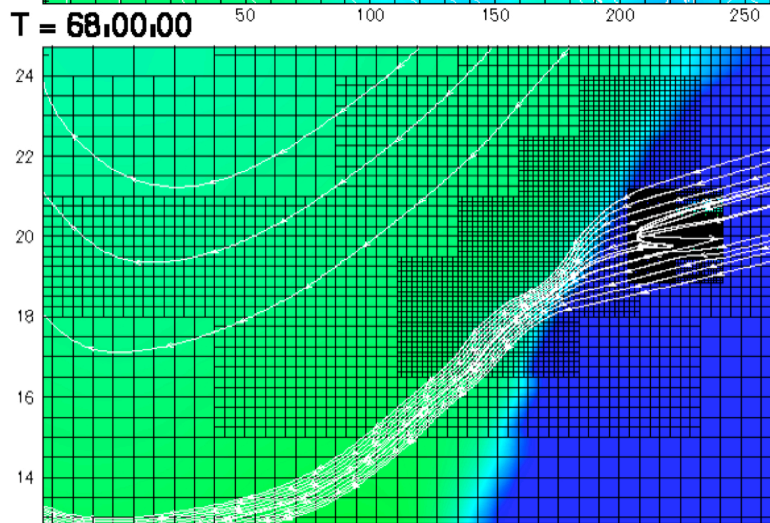
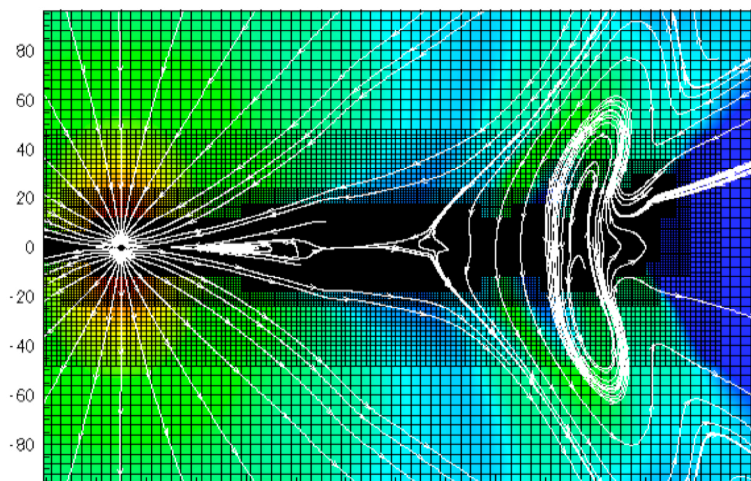
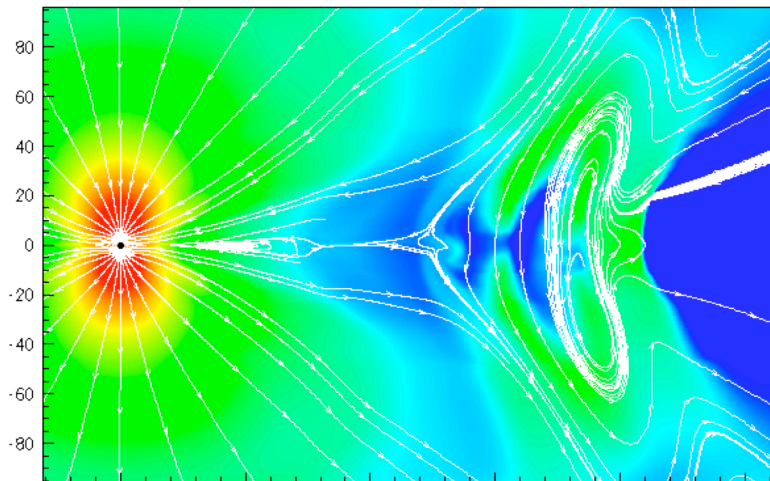
Processes operating at one scale can influence phenomena at other scales.

Image credit: T. Gombosi, CSEM, U of Mich

# Energy moves through the system at a wide range of scales

Where is the Earth in this picture?

stills from the "zoom" movie



- Scales
  - ICME  
few 100 Rs
  - Magnetosphere  
few tenths Rs
- < 0.1% of solar wind particles and <10% of the interplanetary electric field penetrate into geospace

# Internal Geospace Processes

## System Processes

- ✓ Preconditioning
- ✓ Memory
- ✓ Nonlinearity
- ✓ Feedback Loops
- ✓ Instability
- ✓ Emergence

## Main Coupling Processes

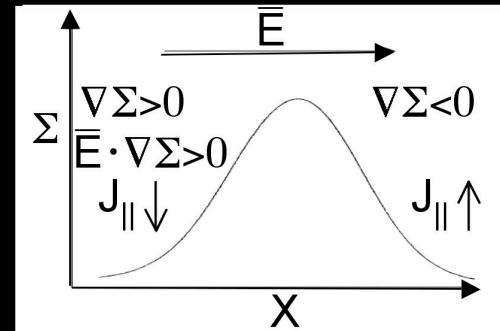
- ✓ Mass / Momentum
- ✓ Plasma - Neutral
- ✓ Chemical - Dynamical
- ✓ Electrodynamical

Cross-scale  
Interactions

# Active Electrodynamic Coupling

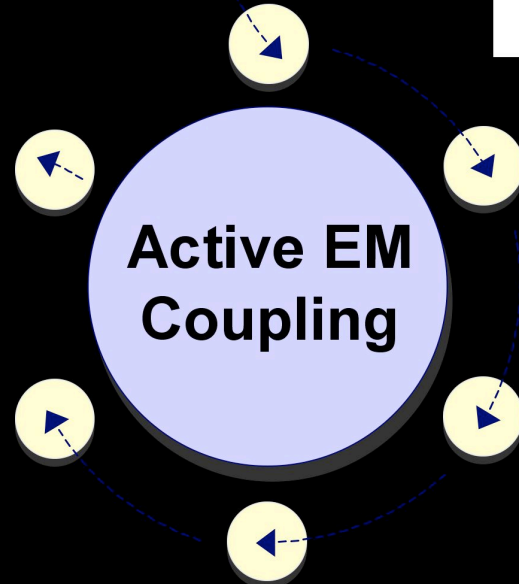
Impose unstructured magnetospheric FAC

Existing conductivity gradients result in ionospheric contributions to FACs



Enhance joule heating & precipitating energy flux

Create small-scale structures in FACs, E-fields



Alfven waves carry FAC information back to magnetosphere

New FACs evolve with associated precipitation

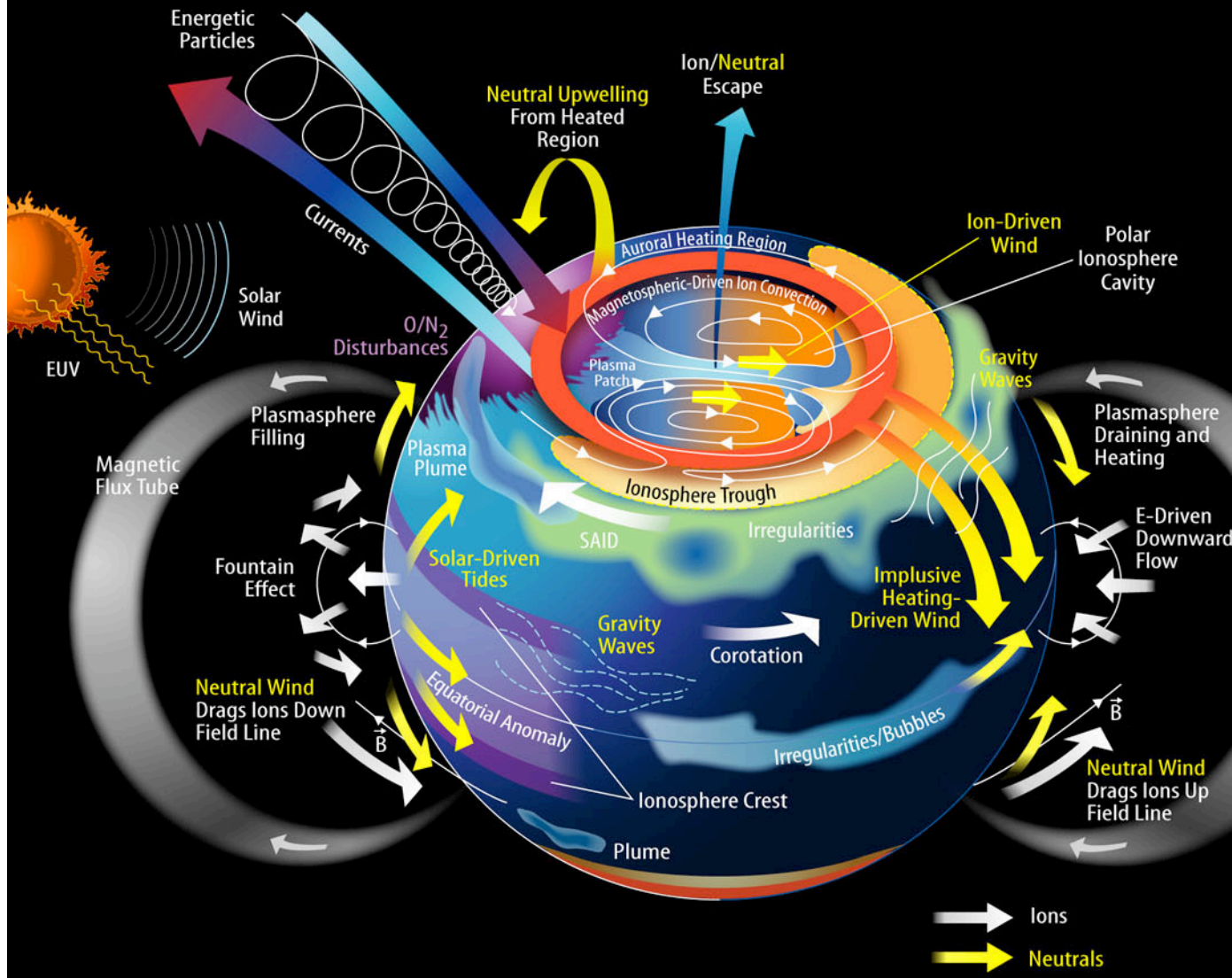
Dynamically-changing conductivity gradients generate new FACs, launch Alfven waves upward

Active electrodynamic coupling is central to the behavior of the Sun-Geospace system, yet the self-consistent patterns of electric fields, currents, and conductivity have never been measured.

Sojka et al., 2006;  
Sojka & Zhu,  
2006; Lotko, 2007

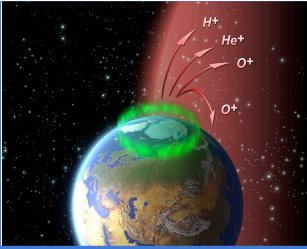
# Ion-Neutral Coupling

Highly structured plasma environment.



- Strength of the interaction proportional to Ne which is controlled by auroral precipitation, solar EUV, chemistry, and transport
- Neutral winds spread local heating globally.
- Heating produces waves that propagate vertically and horizontally.
- Neutral winds:
  - alter the chemistry of the ITM by advecting chemical constituents
  - drag the ions across field lines at low altitudes creating E fields, which alter winds at high altitudes.
  - Seed instabilities at low latitudes.

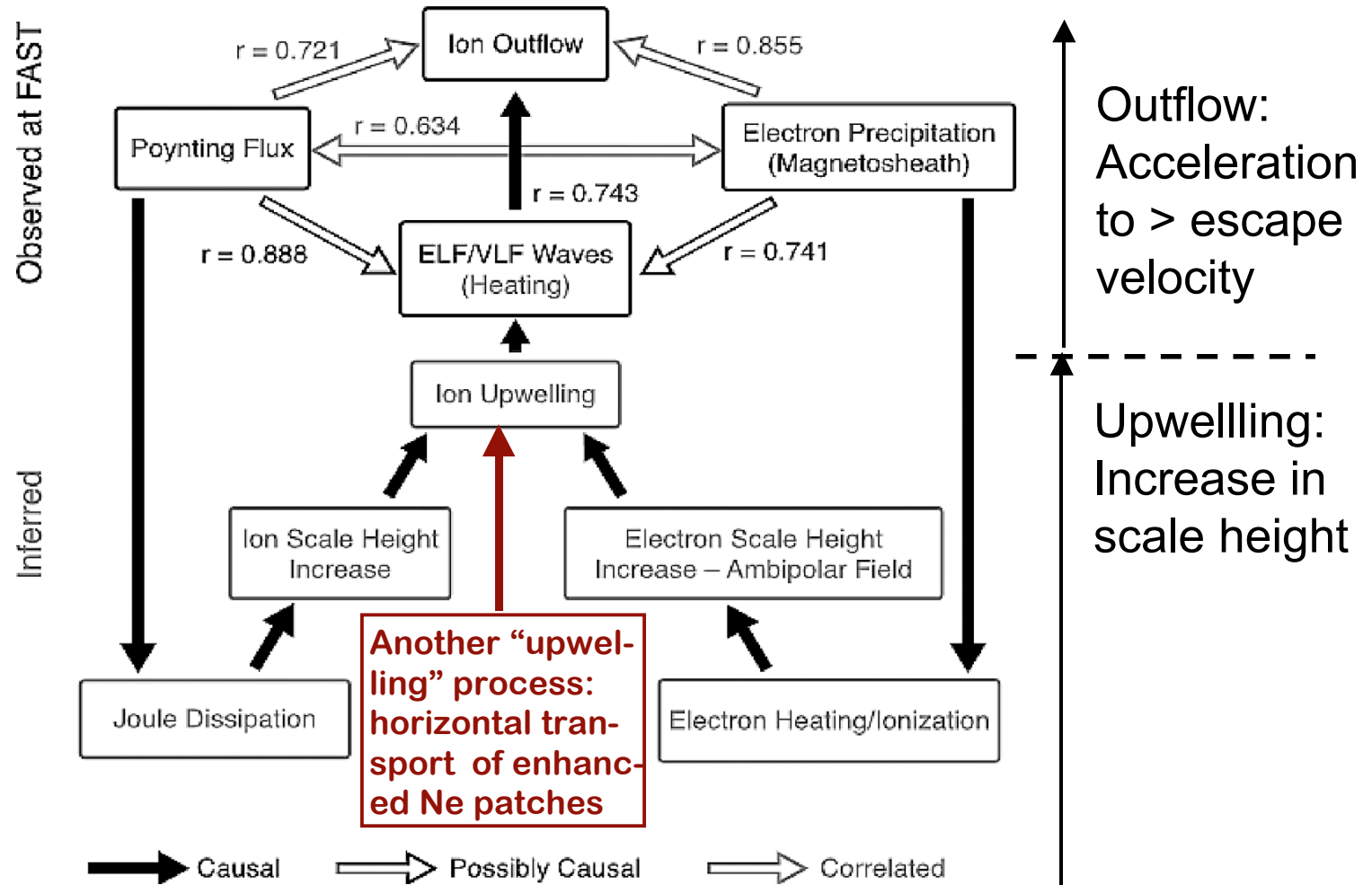
J. Grebow



# Mass / Momentum Coupling

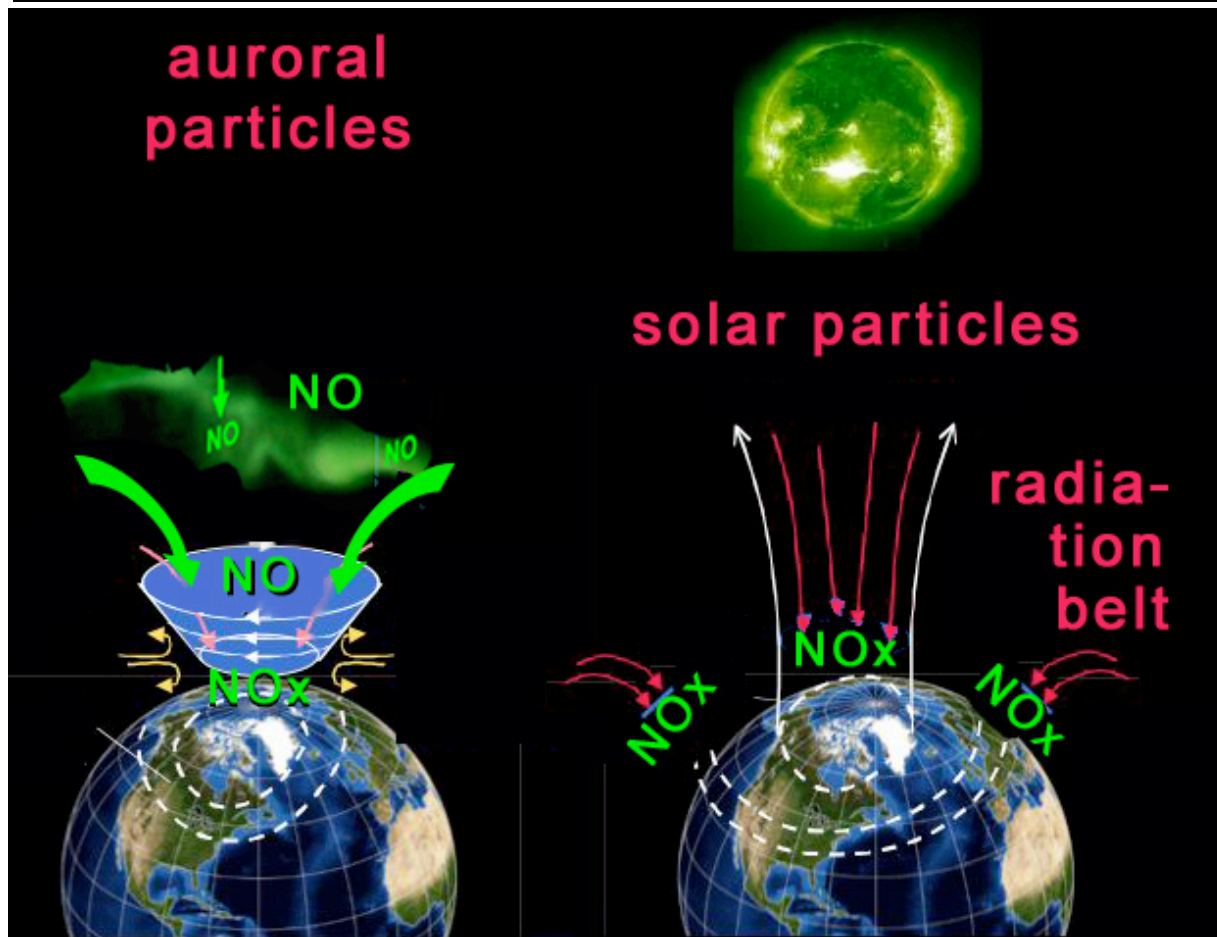
## Ionospheric Outflow: 2-Step Process

Outflows (which involve many independently-driven processes are best correlated with solar wind Pdyn fluctuations: Reason Unknown [c.f. Pollock et al., 1988; Moore et al., 1999]



After Strangeway et al., [2005] as summarized in Moore and Horwitz, 2007 and Lotko, 2007

# Chemical-Dynamical Coupling



Interesting example of coupling between stratospheric meteorology and space weather. [c.f., *Randall et al.*, 2006]. Peaks in NO<sub>x</sub> descent associated with high speed stream activity [*Kozyra et al.*, 2006].

- Upper and lower atmosphere interconnected through chemistry and dynamics.
- Transport of trace and reactive species results in redistribution in atmospheric heating --> dynamical changes
- Energy and momentum also transported by atmospheric waves, such as tides, planetary and gravity waves.
- These waves are forced by the absorption of sunlight in the lower atmosphere, orography, non-linear wave-wave interactions and by latent heat release in clouds.

# Have a feel for geospace as a complex system, now look at interaction sun-to-Earth

- 1) Define the elements of the sun-Earth system.
- 2) Look at the energy budget during a space weather disturbance
- 3) Explore energy inputs to geospace and how they depend on the IMF and other solar wind parameters
- 4) Track geo-effective drivers (and driver combinations) back to their solar sources. Allows us to identify key processes in the Sun's magnetic variability that most dramatically effect Earth. Find links between solar evolution and both short- and long-term variations in the geospace-atmosphere environment. Refine our definitions of geo-effectiveness.

# Geospace Stormtime Energy Budget

- Geospace processes are powered by the sun and solar wind
- Dominant energy input is associated with magnetic merging
- Converted to plasma sheet flows and heating
- Energy is dissipated in:
  - Ring current
  - Auroral particle precipitation and joule heating
- Plasmoids carry energy back to the solar wind

# Energy Budget - 17-21 April 2002 Storms

E (ergs) of Solar eruption		E (ergs) at 1 AU intersecting Geospace cross-section		E (ergs) dissipated in Geospace		E (ergs) radiated to space from the atmosphere	
4/15 & 4/17 CME	-----	Kinetic Energy <sup>3</sup>	$7.3 \times 10^{25}$	Ring Current <sup>4</sup>	$1.0 \times 10^{24}$	5.3 $\mu\text{m}$ NO cooling <sup>6</sup>	$1.4 \times 10^{24}$
$E_p$ 4/21 CME <sup>1</sup>	$5.0 \times 10^{30}$	$\epsilon$ parameter <sup>3</sup>	$3.2 \times 10^{24}$	Joule & Particle <sup>3</sup>	$2.5 \times 10^{24}$		
$E_K$ 4/21 CME <sup>1</sup>	$1.8 \times 10^{32}$			Plasmoids <sup>5</sup>	$1.2 \times 10^{23}$		
4/21 SEP <sup>2</sup>	$3.2 \times 10^{31}$						

<sup>1</sup> Emslie et al., JGR, [2004]

<sup>2</sup> Mewaldt et al., JGR, [2005]

<sup>3</sup> AMIE technique [G. Lu, NCAR]

<sup>4</sup> RAM model [M. Liemohn, UM]

<sup>5</sup> Energy loss due to plasmoids was based on estimate of  $1 \times 10^{22}$  ergs dissipated per substorm [Ieda et al., 1998] and approximately a dozen substorms indicated by the AL index during 17-20 April 2002.

<sup>6</sup> Mlynchzak et al., JGR, [2005, 2006]

# Energy Budget - 17-21 April 2002 Storms

E (ergs) of Solar eruption		E (ergs) at 1 AU intersecting Geospace cross-section		E (ergs) dissipated in Geospace		E (ergs) radiated to space from the atmosphere	
4/15 & 4/17 CME	-----	Kinetic Energy <sup>3</sup>	$7.3 \times 10^{25}$	Ring Current <sup>4</sup>	$1.0 \times 10^{24}$	5.3 $\mu\text{m}$ NO cooling <sup>6</sup>	$1.4 \times 10^{24}$
$E_p$ 4/21 CME <sup>1</sup>	$5.0 \times 10^{30}$	$\epsilon$ parameter <sup>3</sup>	$3.2 \times 10^{24}$	Joule & Particle <sup>3</sup>	$2.5 \times 10^{24}$		
$E_K$ 4/21 CME <sup>1</sup>	$1.8 \times 10^{32}$			Plasmoids <sup>5</sup>	$1.2 \times 10^{23}$		
4/21 SEP <sup>2</sup>	$3.2 \times 10^{31}$	<b>Homework Question: Under typical solar wind conditions, which is greater, the kinetic or magnetic energy and energy flux?</b>					

<sup>1</sup> Emslie et al., JGR, [2004]

<sup>2</sup> Mewaldt et al., JGR, [2005]

<sup>3</sup> AMIE technique [G. Lu, NCAR]

<sup>4</sup> RAM model [M. Liemohn, UM]

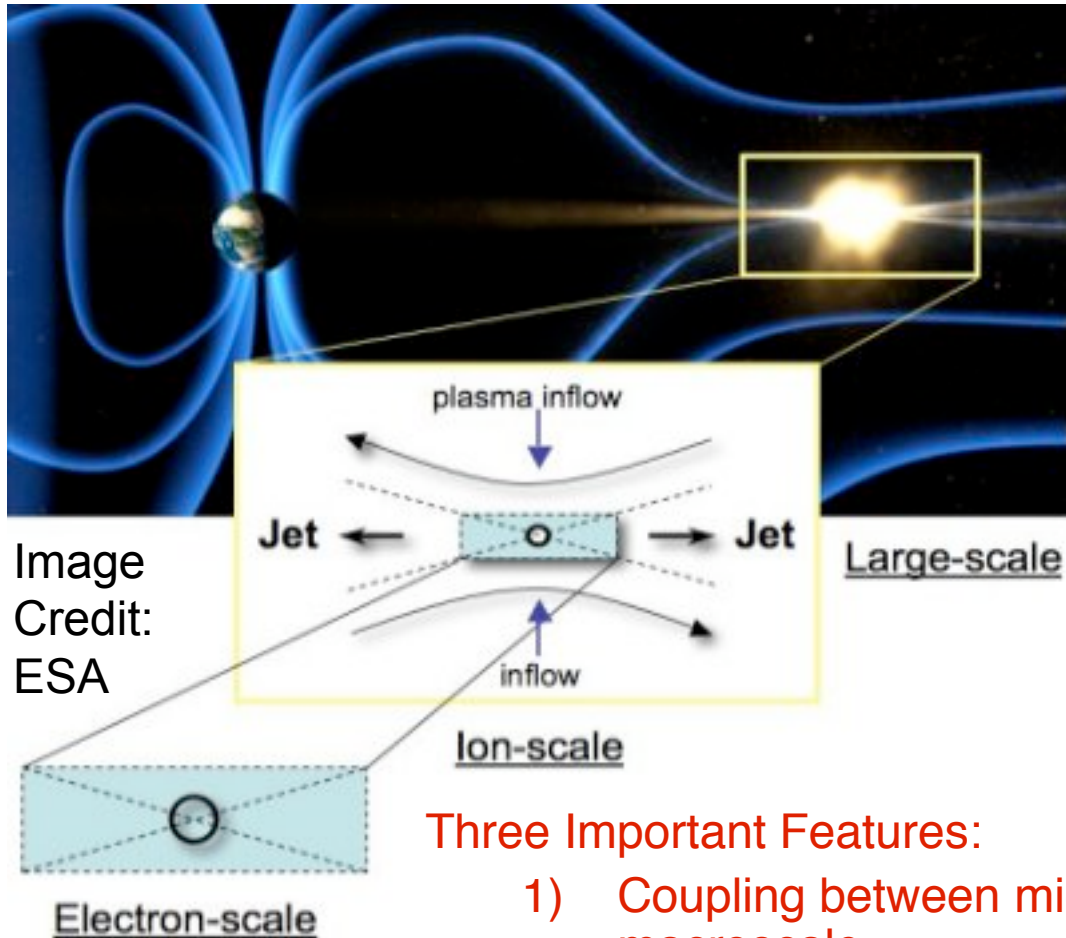
<sup>5</sup> Energy loss due to plasmoids was based on estimate of  $1 \times 10^{22}$  ergs dissipated per substorm [Ieda et al., 1998] and approximately a dozen substorms indicated by the AL index during 17-20 April 2002.

<sup>6</sup> Mlynczak et al., JGR, [2005, 2006]

# Energy Input from the Solar Wind into Geospace

- No direct observations
- Knowledge of energy input based on:
  - Proxies
  - Numerical Experiments with MHD models

# Some basics about magnetic reconnection related to Geospace energy input



DEFINITION [Vaivads et al., *Space Sci Rev*, 2006]:

“Magnetic reconnection is a physical phenomenon where:

- 1) microscopic (*electron and ion gyroradii*) local processes cause a macroscopic change in magnetic topology so that earlier separated plasma regions become magnetically connected,
- 2) on macroscopic (*MHD*) scales the system relaxes to a lower energy state converting magnetic field energy to kinetic energy of charged particles”

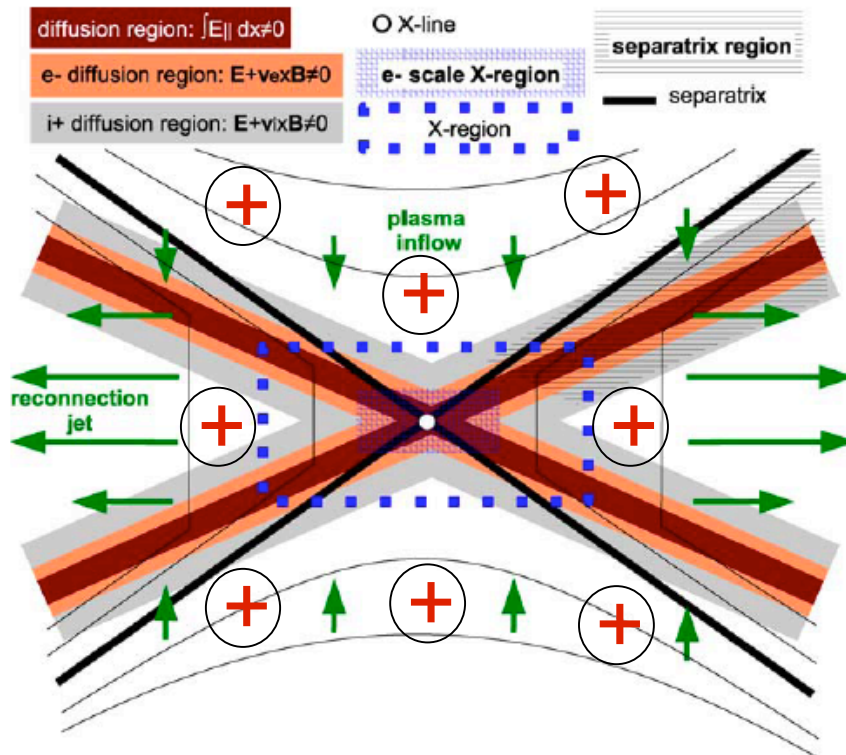
**Three Important Features:**

- 1) Coupling between microscale and macroscale
- 2) Mixing of previously unconnected plasmas
- 3) Conversion of magnetic to particle energy

# Definitions Anti-Parallel Reconnection: Two oppositely directed field lines interconnect. $B = 0$ along the x-line

Vaivads et al., 2006

$\oplus$   $E_{\text{tan}}$



**X-line:** Line along which magnetic field lines from two different topological regions interconnect. In a 2D projection, reduces to a point. Separator, Merging line.

**$E_{\text{tan}}$ :** Electric field locally tangent to the X-line. Determines the transport of magnetic flux to the x-line and the reconnection rate.

**Separatrix:** Surface that separates flux tubes with different topology. 2D projection is a line.

**Separatrix Region:** Broader region around the separatrix where microphysical processes are important.

**Diffusion Regions:** All regions in the separatrix region where topological changes take place. In these regions  $\int E_{\parallel} ds \neq 0$ . Only near the x-line do previously separated field lines become interconnected.

**Guide Field Reconnection:**  $B \neq 0$  along the x-line. In this case  $E_{\text{tan}} = E_{\parallel}$ . Leads to general definition of reconnection  $\int E_{\parallel} ds \neq 0$ , integral is taken along a field line in the reconnection region [c.f., Vaivads et al., 2006].

**Electron (Ion) Diffusion Regions:** Regions in the separatrix region where “frozen-in-flux” condition is broken. Near the x-line, the ion diffusion region is called the X-region and the electron diffusion region is called the electron scale X-region.

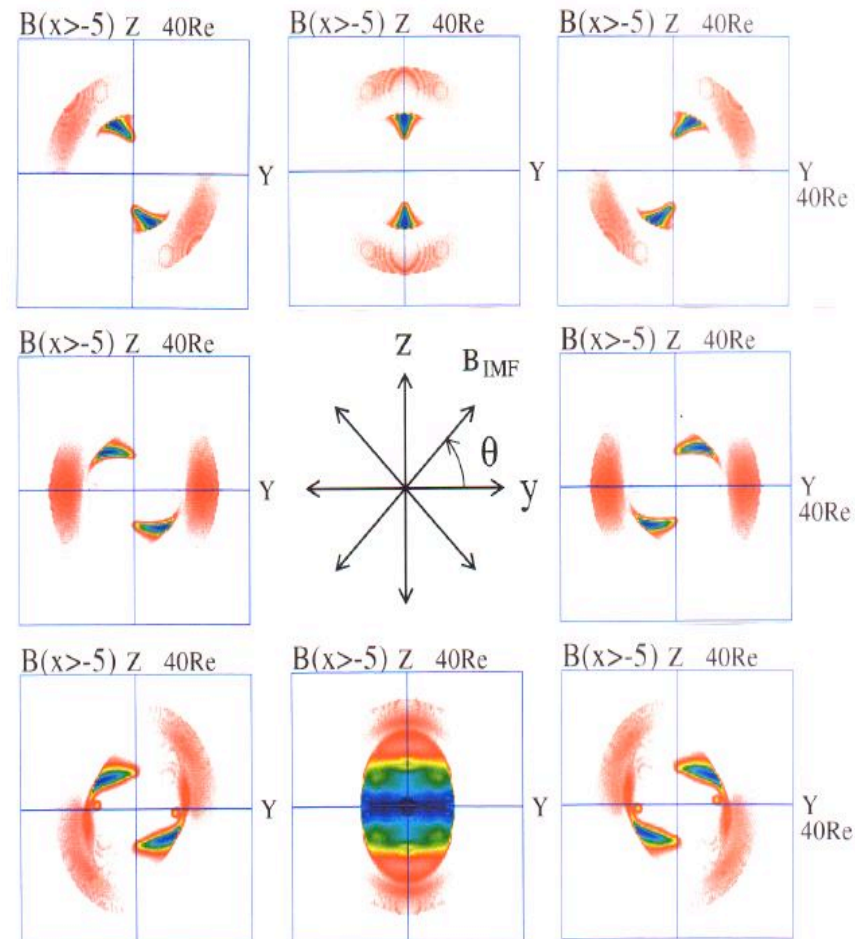
# Anti-Parallel Reconnection vs IMF orientation

- Anti-parallel merging regions for purely horizontal IMF  $B_y$  are located at the high latitude magnetopause on the nightside but move to the high-latitude dayside region equatorward of the cusp and to increasingly lower latitudes with increasing southward IMF component [Crooker, 1979; Luhmann *et al.*, 1984; Ogino *et al.*, 1986; Laitinen *et al.*, 2007].
- This means that two high-latitude merging regions drive magnetospheric convection, one in each hemisphere, rather than the single sub-solar reconnection region during purely southward IMF.
- Anti-parallel merging regions are shifted to the dawnside in the northern hemisphere and duskside in the southern hemisphere for IMF  $B_y < 0$  and the reverse for IMF  $B_y > 0$ .

■ Weak field anti-parallel merging regions

Rotation of incoming IMF

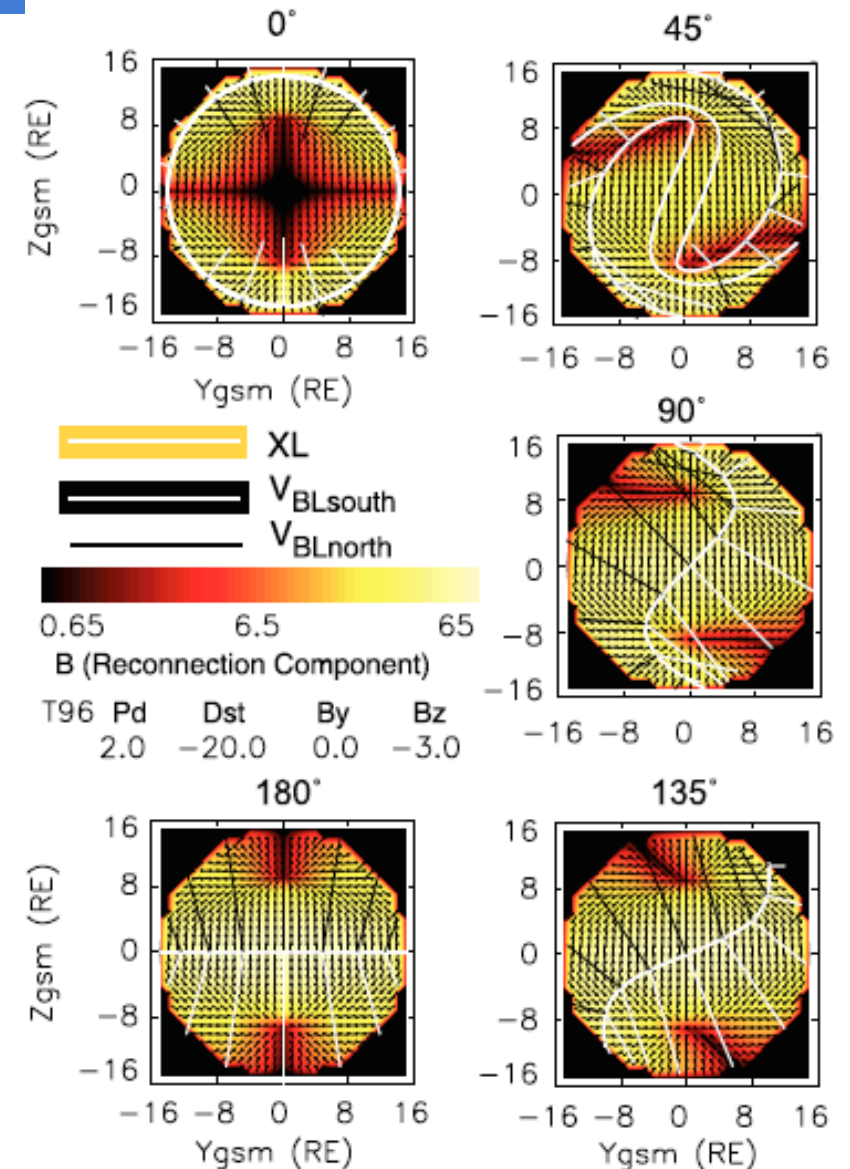
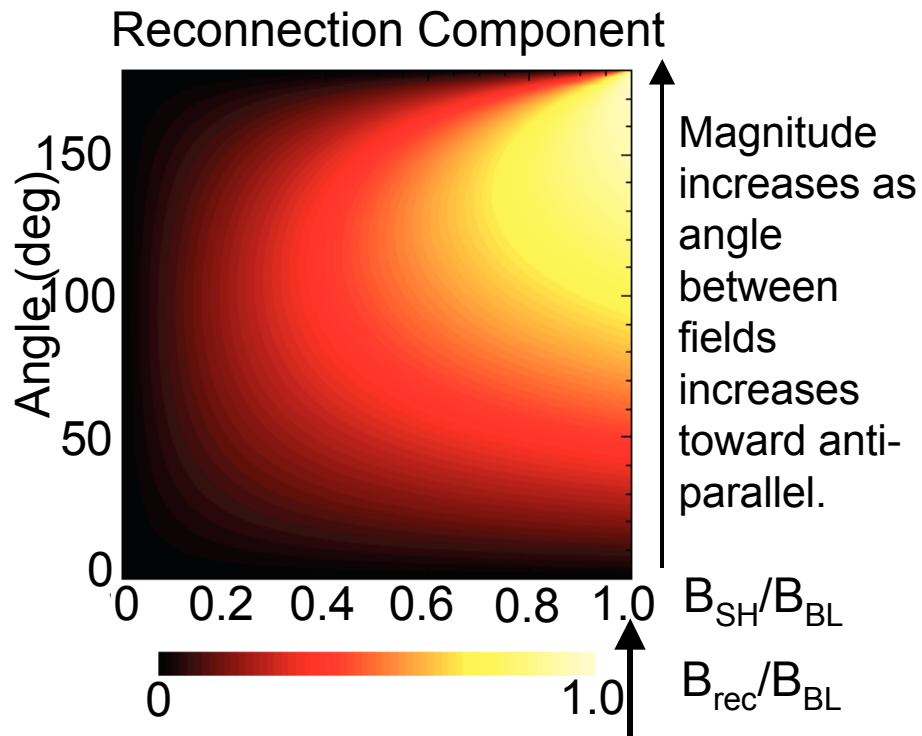
Projection of minimum B region  $B=5.0nT$



<http://center.stelab.nagoya-u.ac.jp/web1/simulation/mhd3d01/fig02.jpg>

# Component Reconnection

Zero tilt,  $B_z = -3\text{nT}$ ,  $P_{\text{dyn}} = 2\text{ nPa}$



- **Component (low shear) Reconnection** [c.f., Moore et al., 2002]: No requirement for anti-parallel reconnection in MHD equations [Cowley, 1976]. X-line is normal to the line along which the two fields have equal and opposite components (called reconnecting component). Different than guide field which parallel to the x-line. Rate goes to zero with the reconnecting components

Moore et al., 2002

# Some Unknowns & Controversies

No observations of total energy input due to reconnection. Critical information for understanding sun-Geospace interaction.

$E_{\parallel}$  distribution in separatrix region and its spatial and temporal variation:

Largely unknown. Some information from simulations. Important in order to understand topological changes in the broader separatrix region and how they relate to the global changes in the magnetic field structure.

How magnetic energy conversion is distributed throughout the separator region and near the x-line: Observations so far are unable to resolve this. Some suggested mechanisms for example are: particle acceleration [c.f., Nagai et al., 2001] and particles interacting with slow shocks [Petschek, 1964]

Vaivads et al., Space Sci Rev, 2006

What you will see in the next slides is that solar wind energy input to the magnetosphere through reconnection (in MHD experiments) takes place over a much broader region than the X-line.



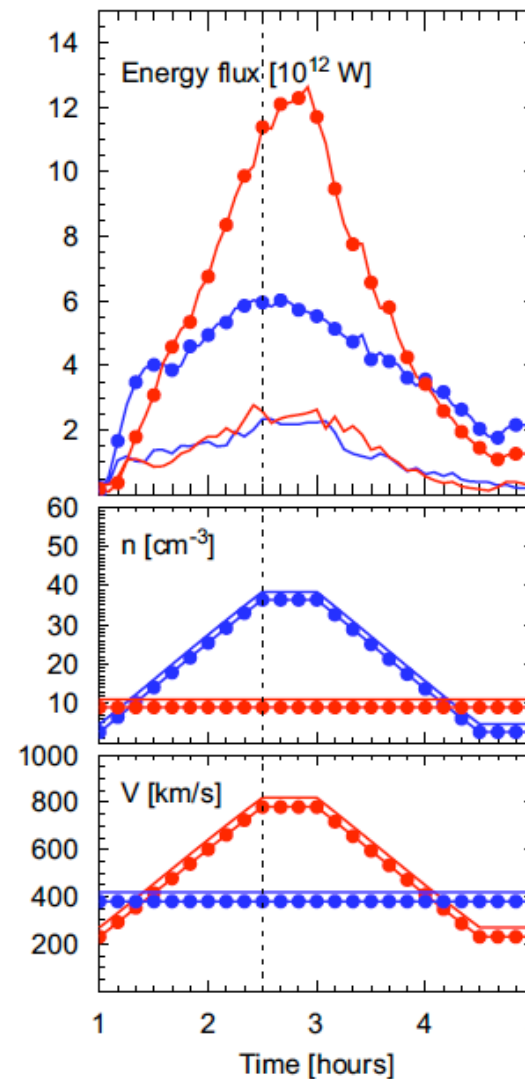
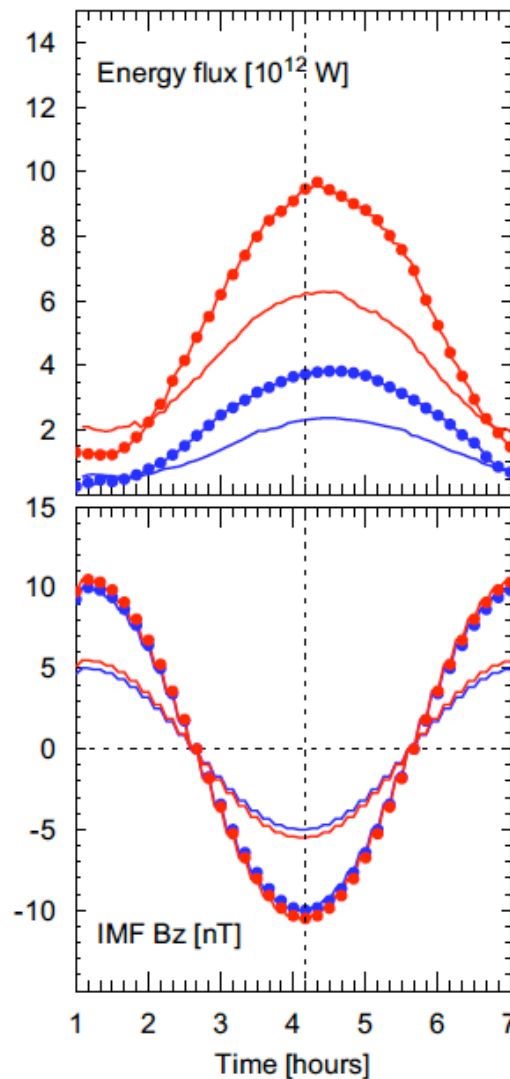
# Energy Input - Dependence on Solar Wind parameters & IMF

High P (8 nPa)

Low P (2 nPa)

● High B  
 — Low B

GUMICS-4  
 MHD  
 Simulations  
 [Pulkkinen et al., JASTP, 2007, 2008; Palmroth et al., 2006]



P = 1-10 nPa  
 by varying:

-  $V_{sw}$  only

-  $n_{sw}$  only

clock  
 angle

● - Bz ( $157.5^\circ$ )  
 — +Bz ( $22.5^\circ$ )

Controlled by  
 reconnection  
 efficiency which  
 depends on IMF,  
 IEF, solar wind  
 density, velocity,  
 pressure

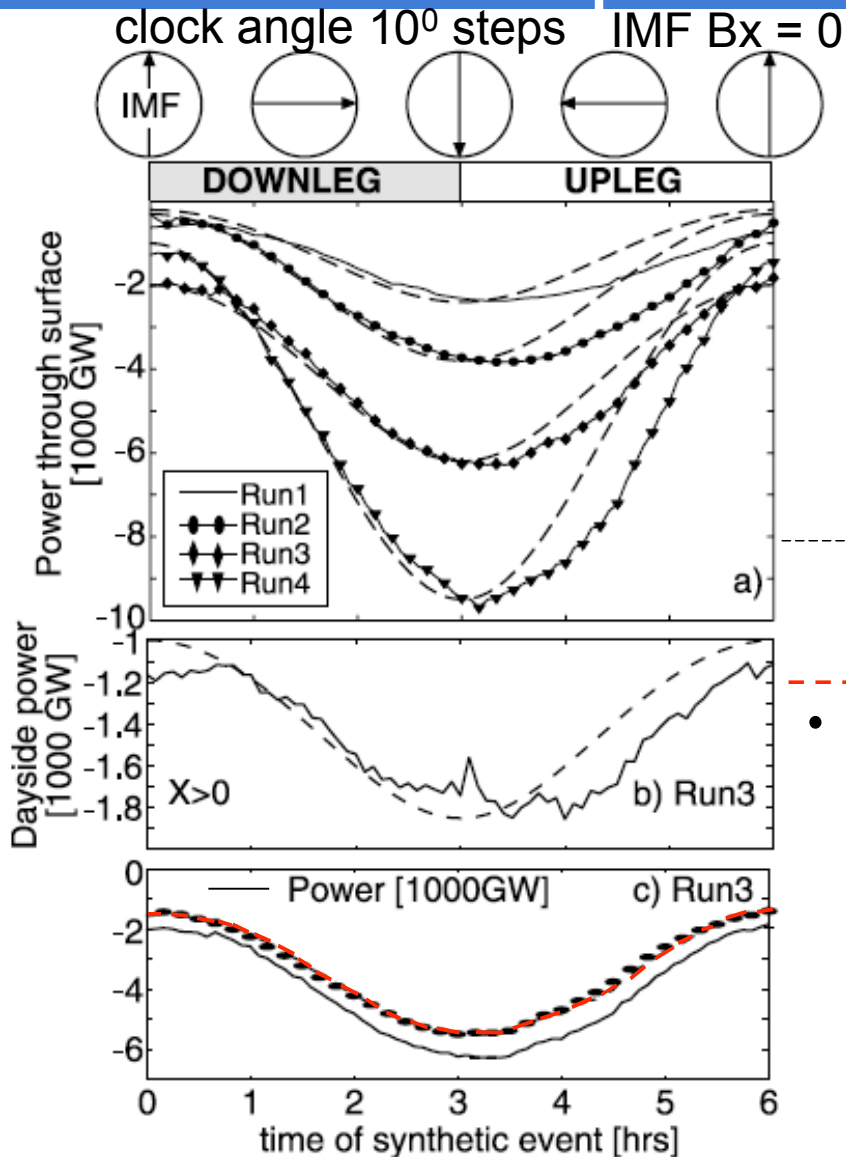
# Energy Input - Dependence on Solar Wind parameters & IMF

	Southward IMF	Northward IMF	Dynamic Pressure
Energy Input	controlled by: <ul style="list-style-type: none"> <li>• IMF orientation and magnitude</li> <li>• Solar wind velocity (more important) and density</li> </ul>	<ul style="list-style-type: none"> <li>• Orientation of IMF is more important than magnitude.</li> <li>• Larger for high speed, low IMF strength</li> <li>• Smaller for low speed, high IMF strength</li> </ul>	<ul style="list-style-type: none"> <li>• Input scales with dynamic pressure</li> <li>• More strongly controlled by solar wind velocity than density for the same pressure</li> </ul>

[Pulkkinen et al., JASTP, 2008]: Overall -- Energy input in simulations controlled by reconnection efficiency with solar wind parameters in order of importance being clock angle and  $V_{sw}$ , followed by  $B$  magnitude and  $N_{sw}$ .

Energy input varies in a manner similar to proxies (like epsilon) but is considerably larger

# History matters. Energy input depends on both present & recent IMF



Power calculated from total thermal, kinetic and electromagnetic energy flux through magnetopause surface to  $x = -30 R_E$ .

Result: Power input proportional to  $\sin^2(\theta/2)$ , when the clock angle rotates from north to south. On the return rotation (south to north) the power input remains enhanced longer than given by  $\sin^2(\theta/2)$ .

scaled  $\sin^2(\theta/2)$

- - - Poynting flux
- Poynting flux using E and B from  $\Delta t$  before through surface from  $\Delta t$  after 03:00 RT

[Palmroth et al., GRL, 2006]

# Characteristic Time Lags & Hysteresis

**Table 1.** Synthetic Run Parameters and Time Lag of Hysteresis

#	$ \text{IMF} $ , nT	$p_{dvn}$ , nPa	Time Lag, min
1	5	2	30
2	10	2	40
3	5	8	20
4	10	8	30

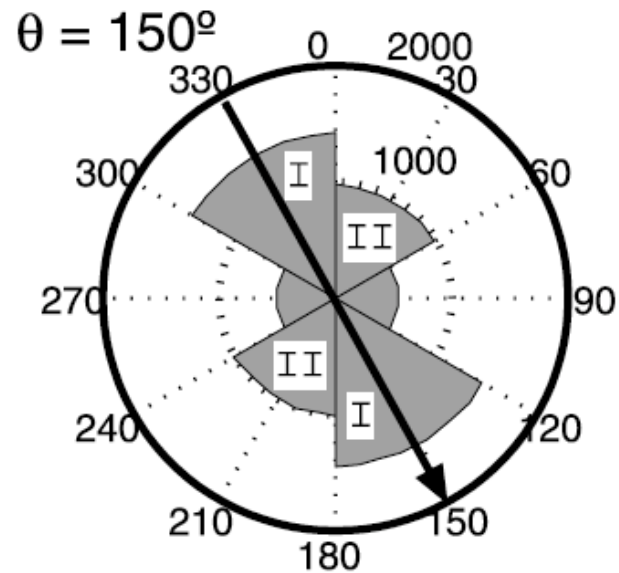
\*The time lag computed by finding the best correlation for delayed upleg power transfer with the upleg  $\sin^2(\theta/2)$

The energy input *after* an interval of southward IMF is stronger than for the same conditions *before* the southward IMF interval.

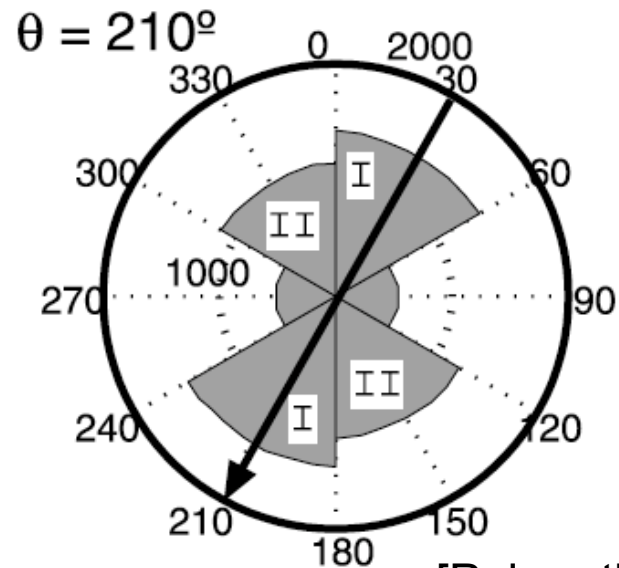
After the IMF rotates to a new value, there is a change in reconnection within 10-15 minutes [Laitinen et al., 2007] and a response in the energy input through the magnetopause within 20-40 minutes [Palmroth et al., 2006].

This time delay can be comparable to the time between significant IMF rotations (for example, in high-speed streams).

# What causes the hysteresis?



Input power from run #3 integrated over  $x$  and plotted vs azimuth angle radially from 0 to 2000 GW at the outer circle. Clock angle marked by arrow.



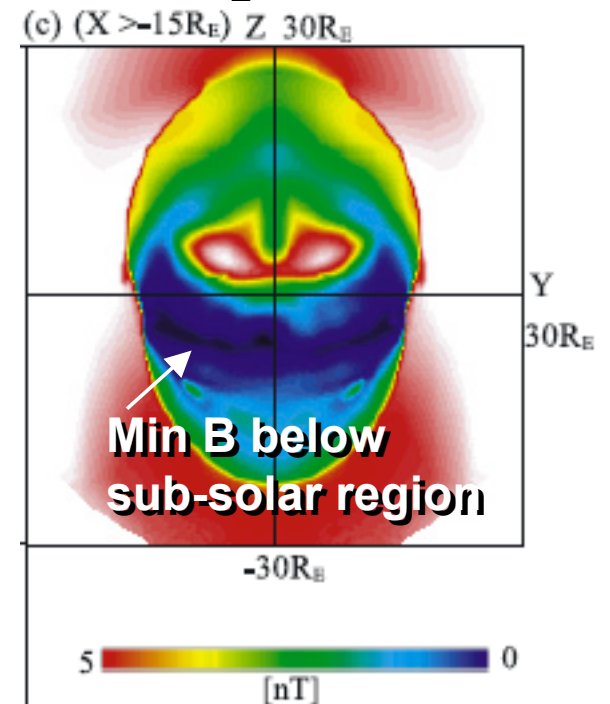
Cause of Hysteresis: Power input remains high in regions associated with recently visited clock angles (region II). Reason not yet known.

[Palmroth et al., GRL, 2006]

# Energy input also depends on dipole tilt

- Dipole tilt varies with UT and season. It defines the geometry between the internal geomagnetic field and IMF
- Controls the polar cusp location [Zhou and Russell 1997].
- Shifts reconnection away from the sub-solar point [c.f., Maynard et al., 2002,2003; Park et al., 2006]. Reconnection rate is smaller because of increased magnetosheath flows [Park et al., 2006]

Projection of magnetic field magnitude for  $X > -15 R_E$



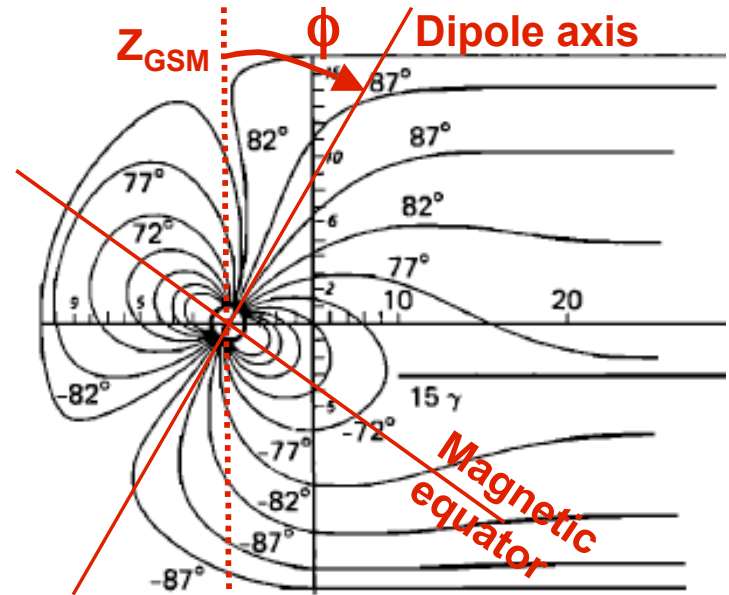
MHD simulation,  
purely southward  
IMF,  $30^\circ$  dipole tilt

Park et al., 2006

# Dipole Tilt

Angle between the Earth's north dipole axis and the  $Z_{GSM}$  direction. Positive for tilts toward the sun

Question: How does the dipole tilt vary over a day and over the year? Does this mean that magnetic activity can have a UT dependence?



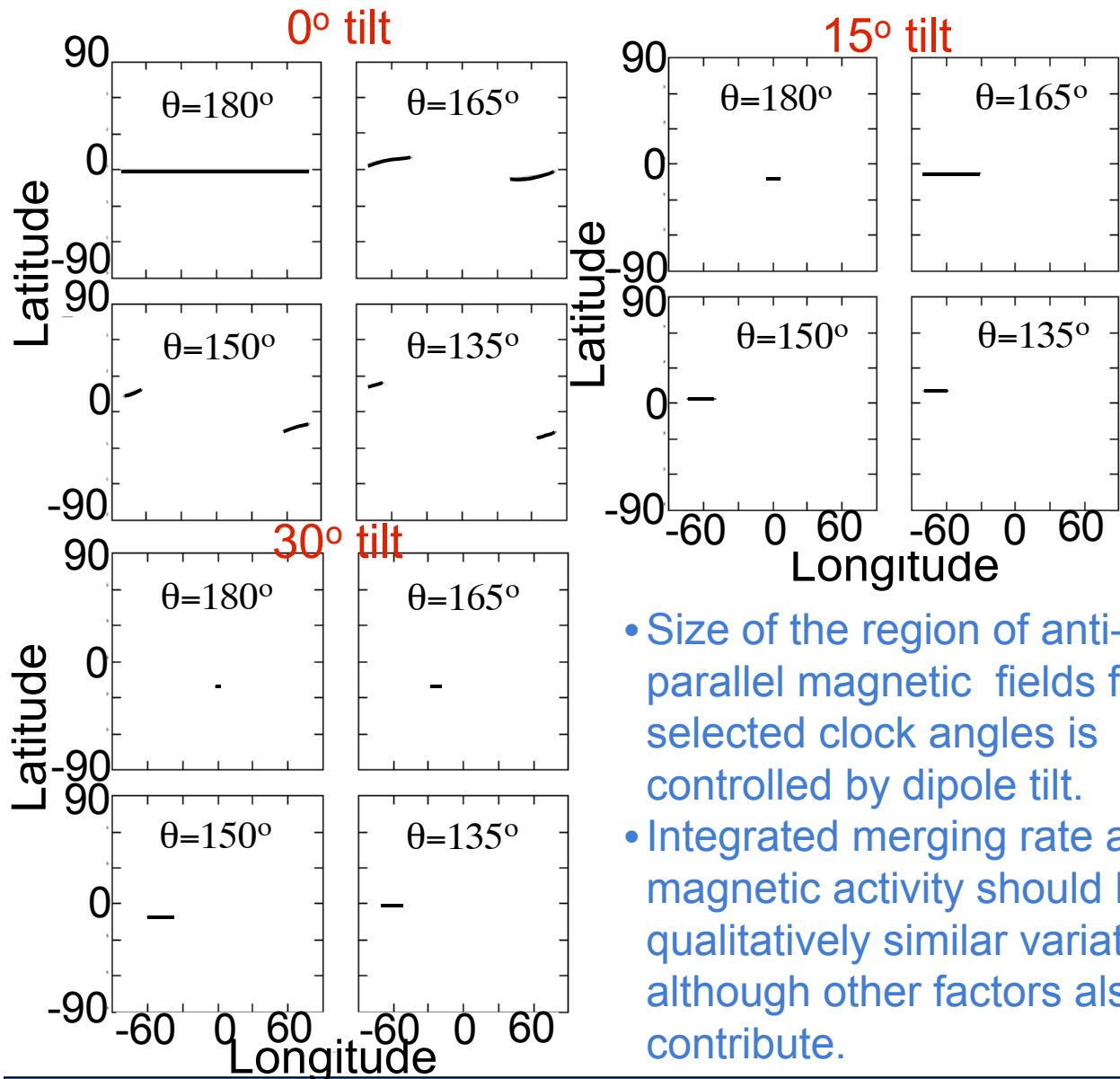
$$\Phi_{day} = 9.4 \cos \left[ (UT - 17.29) \frac{2\pi}{24} \right], \quad \text{Shue et al., GRL, 2002}$$

$$\Phi_{year} = 23.4 \cos \left[ (DOY - 172) \frac{2\pi}{365.25} \right],$$

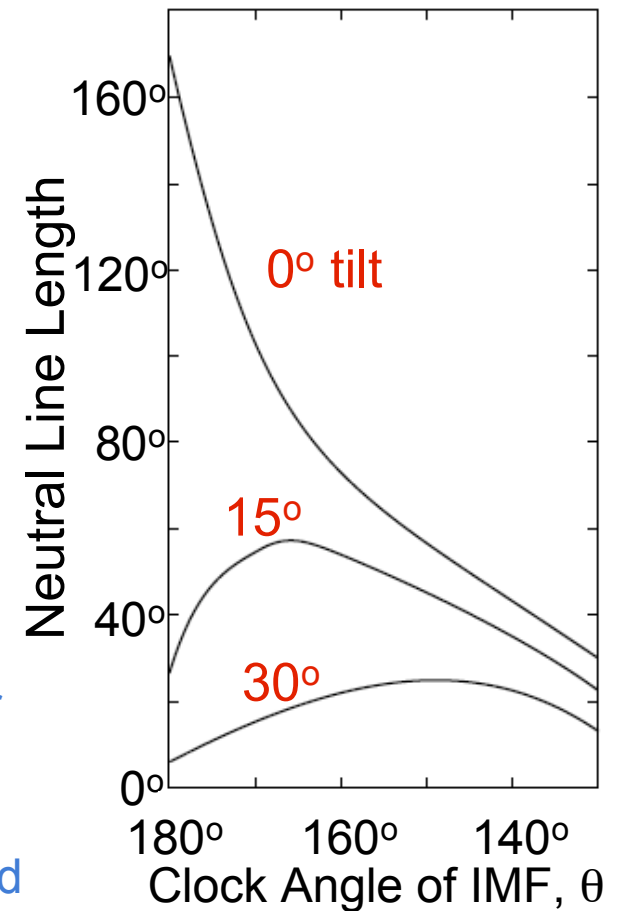
$$\Phi_{tilt} = \Phi_{year} + \Phi_{day}.$$

Shue, PhD Thesis, 1993;  
Nowada et al., Planet. Space Sci., 2009

# Dipole tilt may effect anti-parallel merging



- Size of the region of anti-parallel magnetic fields for selected clock angles is controlled by dipole tilt.
- Integrated merging rate and magnetic activity should have qualitatively similar variations although other factors also contribute.

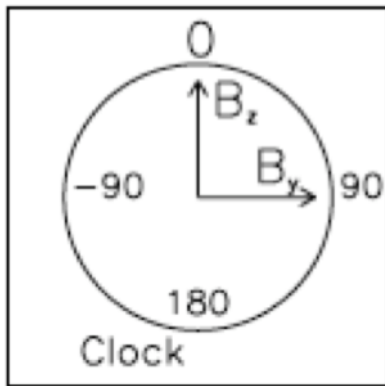


Russell et al., GRL, 2003

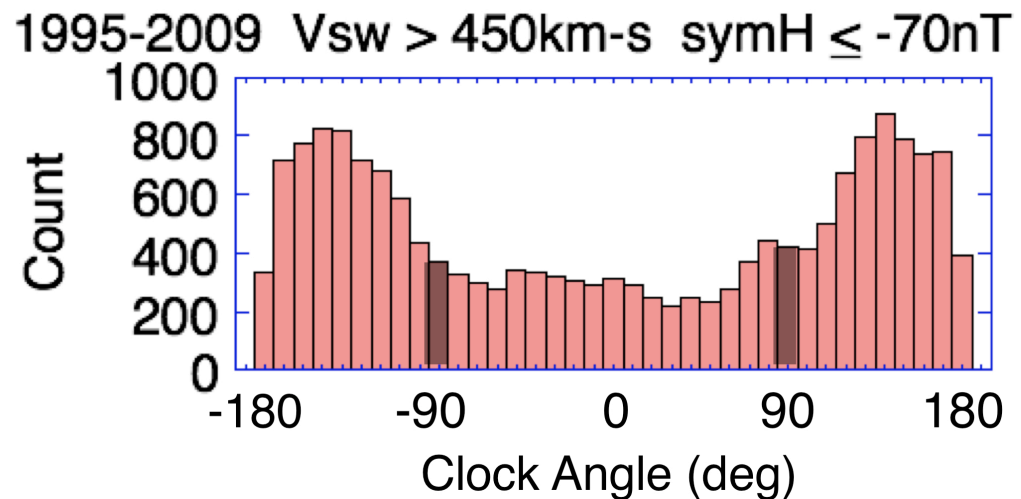
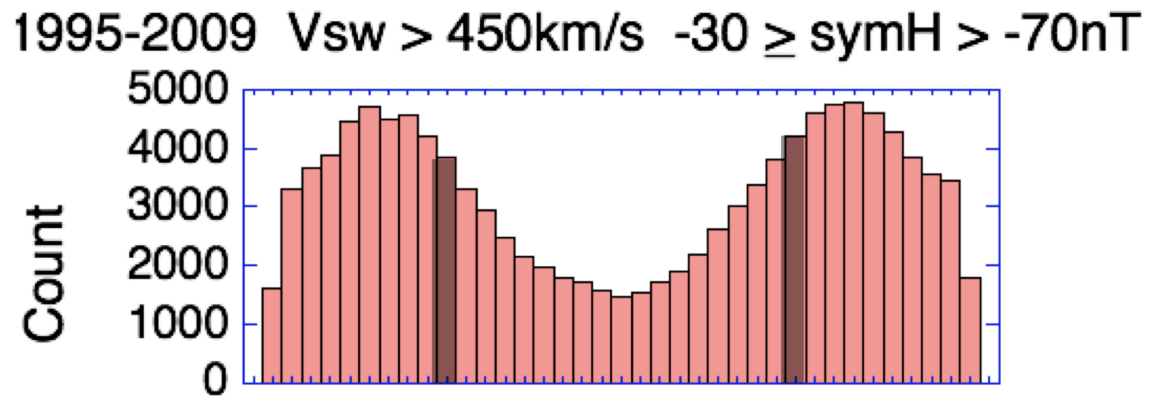
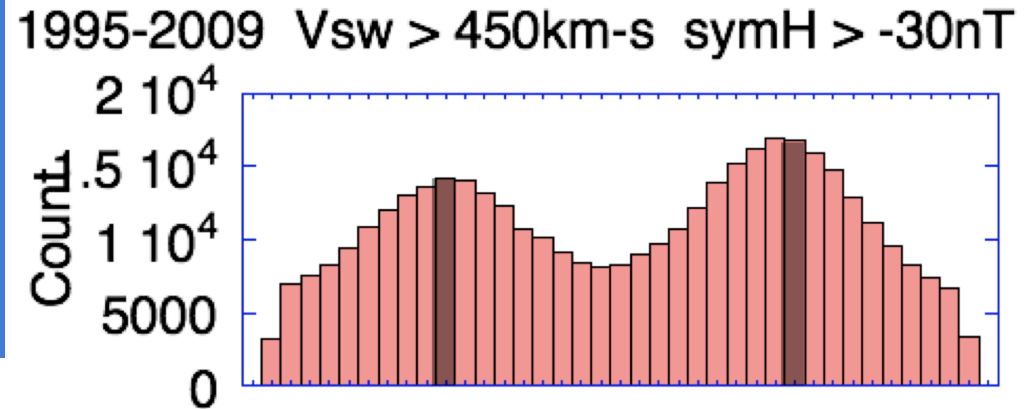
# *Geospace Response* is strongly dependent on IMF Direction

- Reconnection happens where
  - IMF is ~anti-parallel to the magnetospheric field and convection drives the fields together.
  - Component reconnection in the sub-solar region can also play an important role.
- The orientation of the IMF has a major impact on
  - magnetospheric configuration
  - plasma populations
  - resulting magnetic activity.
- Allow solar wind mass and energy to enter the magnetosphere
- Results in large-scale circulation of plasmas and field lines results.
- Provides energy that powers all types of magnetic activity.

# Direction of IMF during Active Times



Oblique IMF is most common orientation

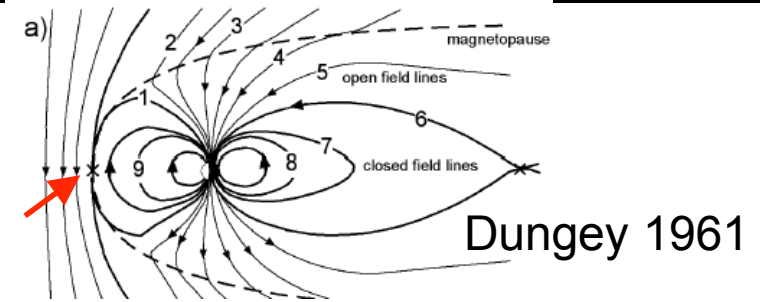


# Effects of IMF Direction on the Geospace System

## Southward IMF

*Unique feature:*  
most effective solar  
wind energy  
transfer

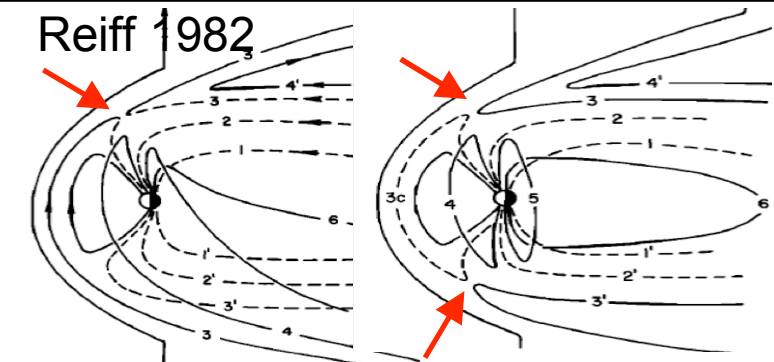
Subsolar anti-parallel merging  
region. Reconnection rate is  
greatest here where magneto-  
sheath flows are slowest [c.f.,  
Park et al., 2006].



## Northward IMF

*Unique feature:*  
enables capture of  
large amounts of  
solar wind plasma  
[c.f., Li et al., 2008]

Poleward-of-cusp merging.  
Solar wind/magnetosheath  
capture occurs when merging  
takes place either simultaneously  
in both hemispheres or  
sequentially.



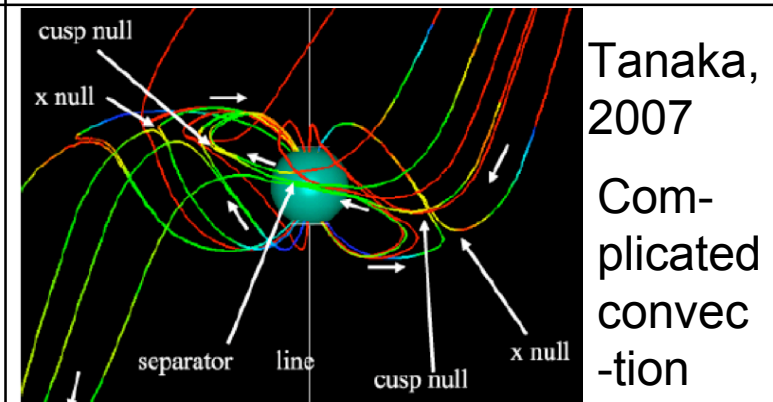
## Oblique IMF

(strong IMF  $B_y$   
with small  $B_z$ )

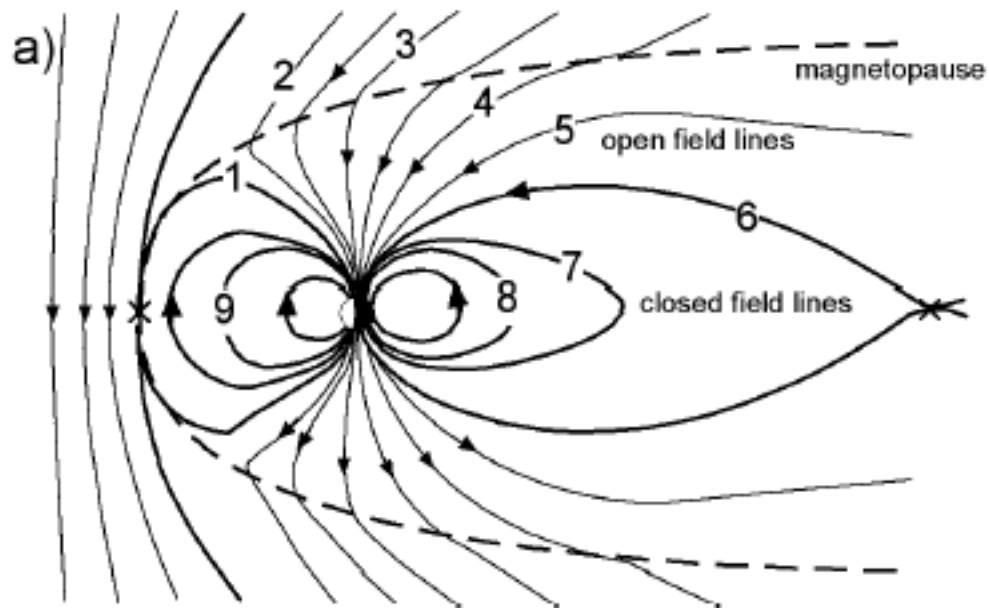
*Unique feature:*  
multiple merging  
regions operating  
simultaneously

Five merging regions:

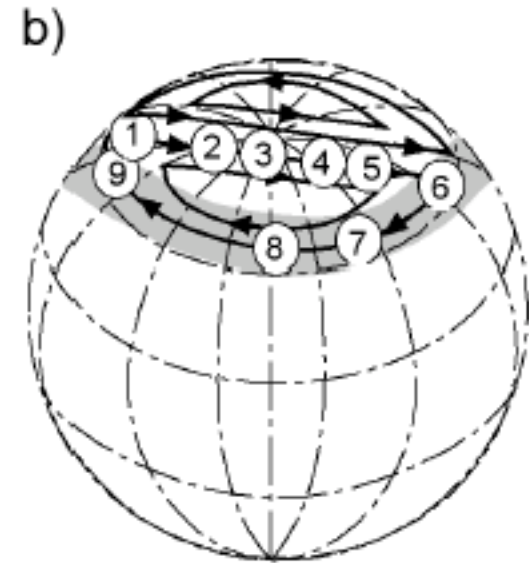
- 2 anti-parallel high-latitude (cusp null)
- 2 poleward of cusp (x null)
- 1 sub-solar (component merging)



# How does Southward IMF drive the geospace system?



2-cell convection pattern. Drives anti-sunward convection over the polar cap



After Dungey [1961]. Figure from Palmroth [2003]

Treated in more detail in V. Vasiliunas lecture

# Geospace Response - Southward IMF

[c.f., Gonzalez et al., 1994, and references therein]

- Strong long-lived dawn-dusk electric fields associated with the passage of strong southward IMF by the Earth are the primary cause of magnetic storms.
- Energy is transferred to the magnetosphere via magnetic reconnection. [Treated in V. Vasiliunas lecture]
  - Efficiency of the energy transfer  $\sim 10\%$  for strong magnetic storms [Gonzalez et al., 1989]
- Convects plasma deep into the inner magnetosphere. Along the way it is adiabatically and non-adiabatically energized to form the stormtime ring current. [See M. Liemohn lecture later this week].
- Solar wind dynamic pressure enhances the geo-effectiveness.

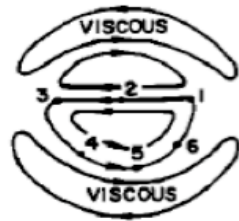
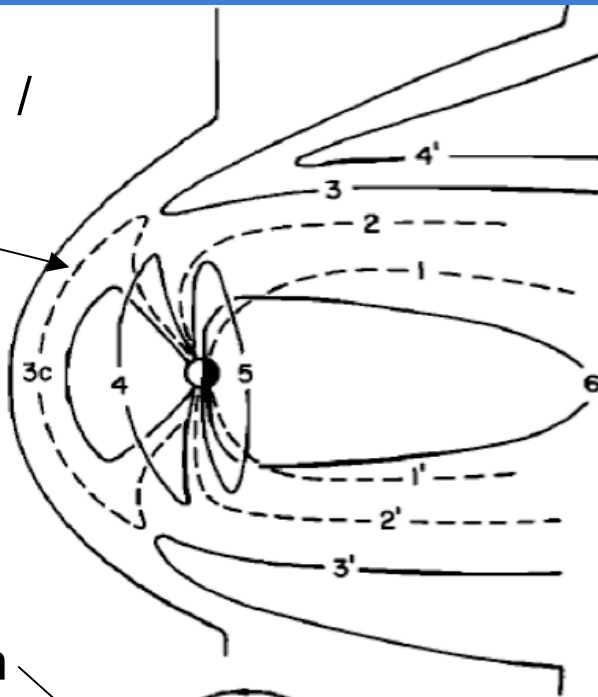
**Table 1.** ( $B_z$ ,  $\Delta T$ ) Thresholds for Storms at 80% Occurrence Level (ISEE 3 Interval: August 1978 to December 1979)

	$Dst$ , nT	$B_z$ , nT	$\Delta T$ , hours
Intense	-100	-10	3
Moderate	-50	-5	2
Small (typical substorm)	-30	-3	1

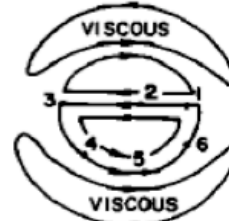
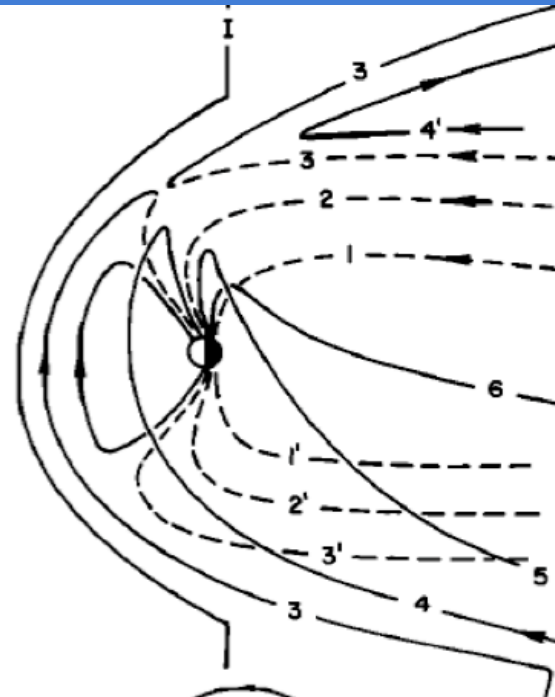
# How does northward IMF drive the Geospace system?

Solar wind /  
magneto-  
sheath  
plasma  
captured  
on closed  
field lines.

4-cell  
convection  
pattern.  
Drives  
sunward  
convection  
over the  
polar cap

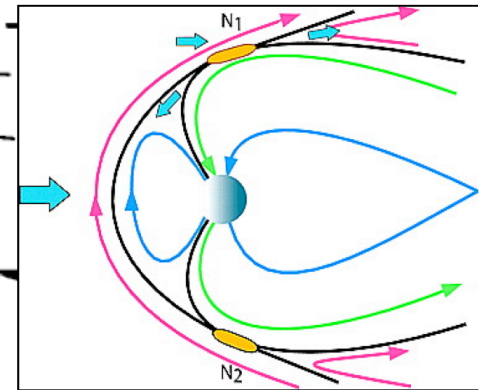


After Reiff, JGR, 1982

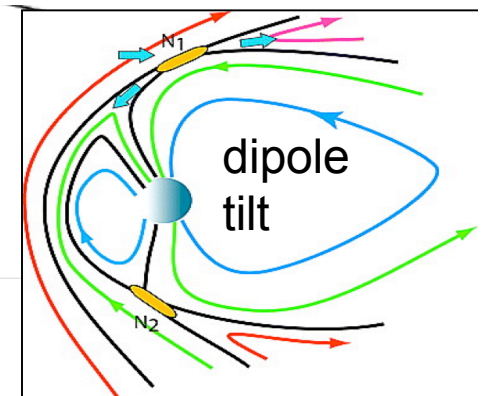


After Dorelli et al., JGR, 2007

Simultaneous high-  
latitude reconnection



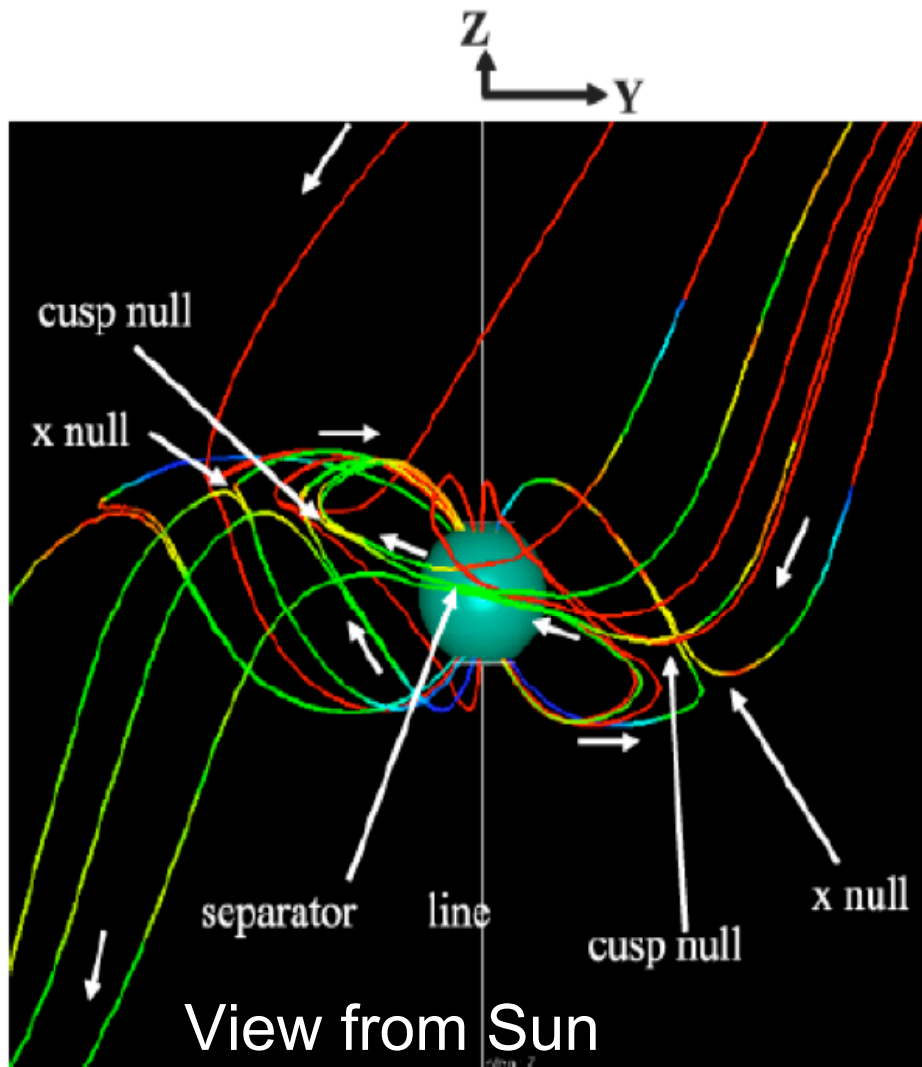
Sequential high-  
latitude reconnection



# Geospace Response - Northward IMF

- During strongly northward IMF, simultaneous or nearly simultaneous double high-latitude reconnection results in a large rate of mass transfer from the solar wind into the closed field line region of the magnetosphere. [c.f., *Øieroset et al.*, 2005, 2008; *Lavraud et al.*, 2006; *Li et al.*, 2005, 2009; *Watanabe et al.*, 2006; *Laitinen et al.*, 2007]
- This efficient mass transfer results in the formation of cold dense plasma sheets and the capture of stagnant solar wind plasma inside the dayside magnetopause.
- Some system effects:
  - Evidence that the addition of cold dense plasma to the dayside magnetopause region influences the reconnection rate [c.f., Borovsky and Denton, 2006; Borovsky et al., 2008].
  - Cold dense plasma sheet provides a particularly effective source population for the ring current that can be delivered to the inner magnetosphere during subsequent southward turnings of the IMF [c.f., *Thomsen et al.*, 2003; *Lavraud et al.*, 2005,2006]

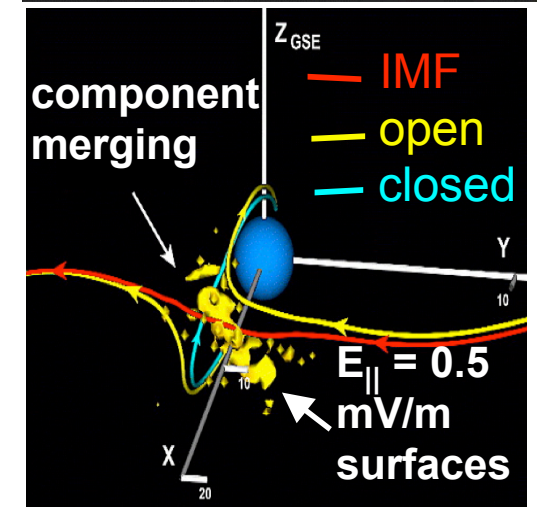
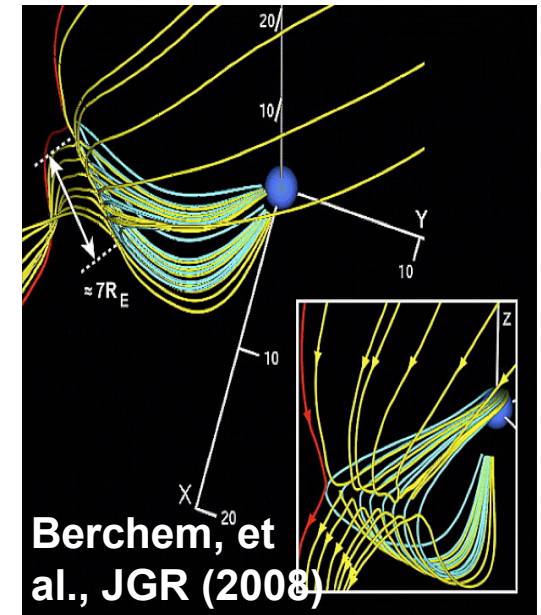
# How does oblique IMF drive the Geospace system?



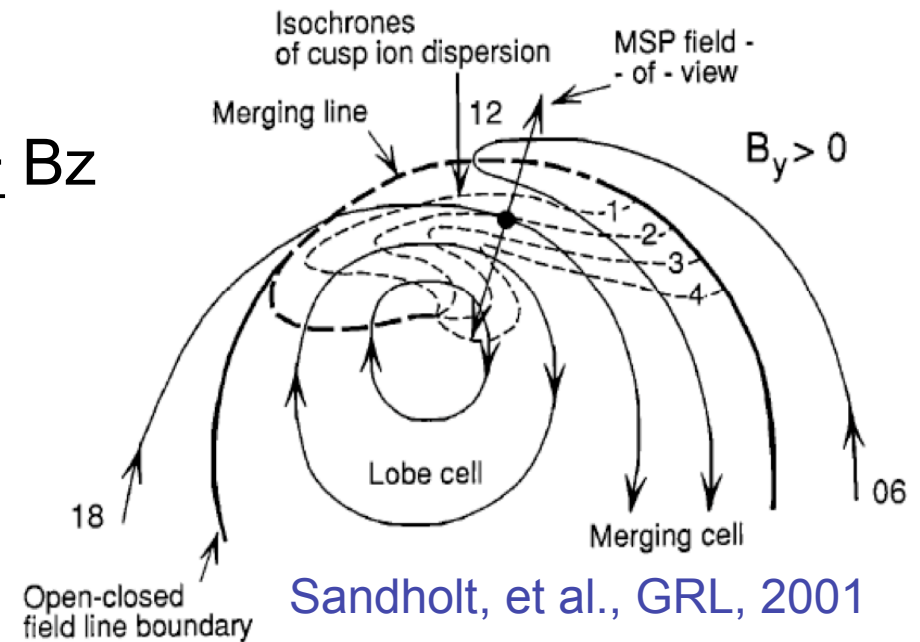
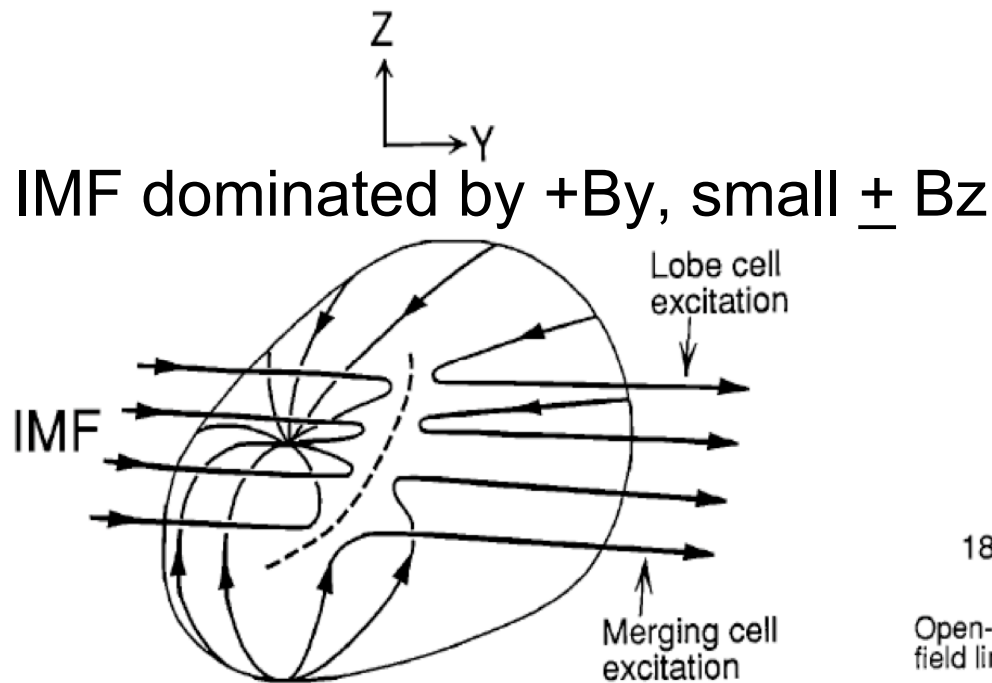
Tanaka, Space Sci Rev, 2007

- 5 merging regions: a sub-solar component and four anti-parallel high-latitude merging sites
- Shows field lines near the open-closed boundary
- Separator line is the 3D analogue of 2D x-lines.
- White arrows show B field direction

Views from OPEN-GGCM

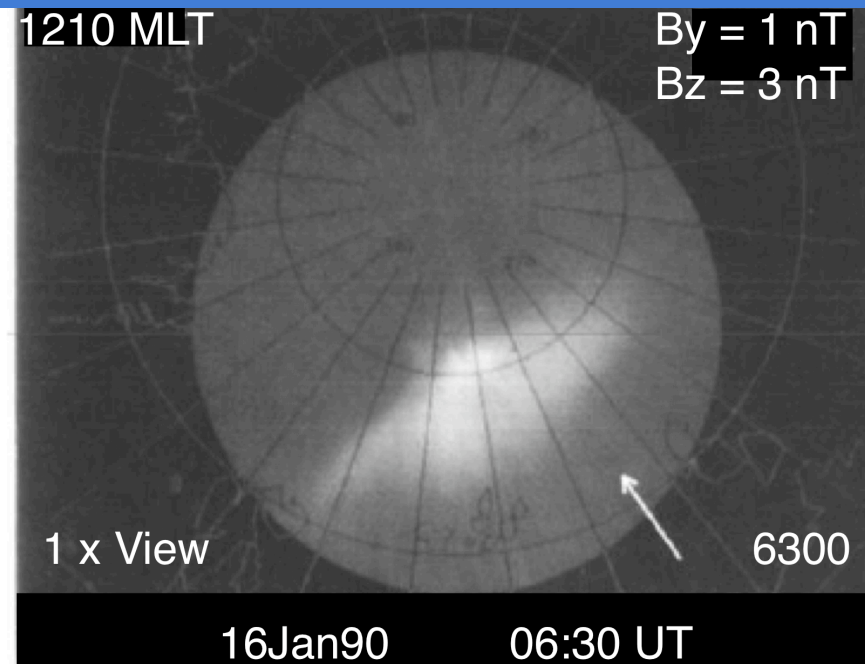
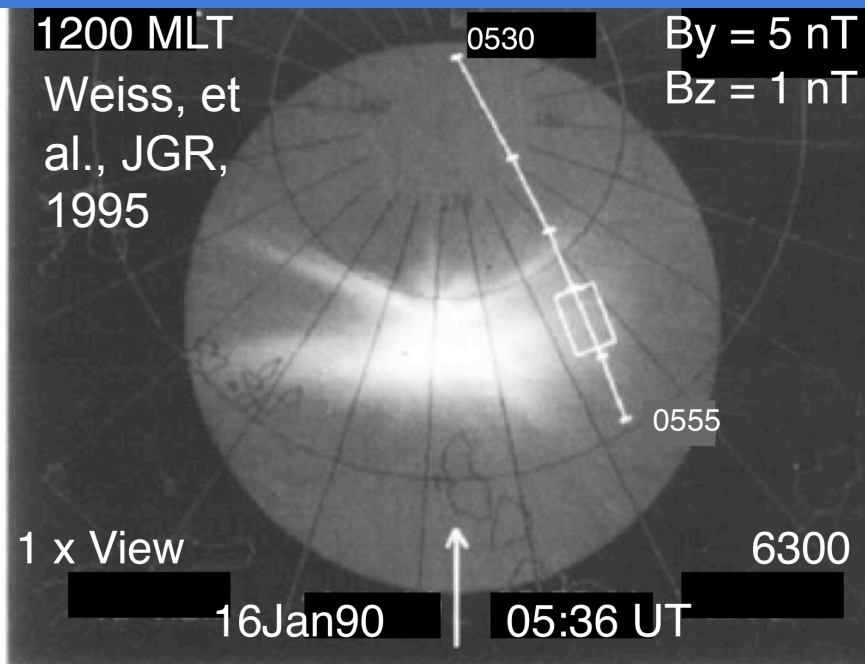


# Convection patterns under oblique IMF



- Magnetic tension (resulting from kinks in the field lines introduced during the reconnection process) drags the field lines westward towards noon for negative IMF  $B_y$  and the reverse for positive IMF  $B_y$ .
- As field lines move in the dawn-dusk direction, they become less kinked and by the time they approach noon MLT they are moving largely tailward with the solar wind flow [e.g., Smith and Lockwood, 1996].
- This initial dawn-dusk motion of the field line creates an east-west dispersion in the energy of precipitating ions [Weiss et al., 1995; Wing et al., 2001].

# Visible evidence of the change of convection during oblique IMF compared to southward IMF



- Obliquely southward IMF conditions are statistically associated with the appearance of a cold dense ion population at geosynchronous orbit on the dawnside [Lavraud et al., 2006]. This is a separate population from the cold dense plasma sheet that appears near midnight after northward IMF intervals. Do multiple reconnection sites re-close open flux tubes to capture solar wind plasma?
- Oblique IMF is typical of high-speed streams, in which *fluctuating* magnetic fields from Alfvén wave trains are superimposed on a Parker spiral IMF configuration --> Hysteresis and transition between states.

# To summarize so far ....

- Energy input to geospace depends on (1) solar wind parameters, IMF strength and orientation and (2) dipole tilt.
- Each major IMF orientation (north, south, oblique) brings with it unique geospace consequences.
  - **Southward IMF:** Most effective solar wind energy transfer. Drives strong magnetic activity
  - **Northward IMF:** Captures large amounts of solar wind plasma on closed field lines. Produces cold dense plasma sheets which can be delivered into the inner magnetosphere if the IMF turns southward
  - **Oblique:** Multiple merging regions. Results in complicated convection patterns.
- Hysteresis occurs. Energy input depends on both present & recent IMF
- Simulations indicate that the magnetosphere takes 10-15 minutes to reconfigure and activate new merging sites. There is a time delay of 20-40 to reach maximum energy input after a change in the IMF.
  - Variations in solar wind and IMF parameters on shorter time scales (i.e.. In high speed streams and shocks) may mean the magnetosphere is in transition between known configurations a large part of the time

Trace back through system from geospace  
to Sun to identify geo-effective solar &  
heliospheric processes

# Geoeffectiveness: Primary Parameters

## Basic Parameters

- Simulations indicate that solar wind energy input controlled by:
  - IMF strength & orientation (pure IMF  $B_{\text{south}}$  most effective),
  - $V_{\text{sw}}$ : high values intensify interplanetary electric field, drive strong shocks that accelerate solar particles
  - Dynamic pressure ( $V_{\text{sw}}$  more important than  $N_{\text{sw}}$  for a given pressure)
- Geoeffective solar wind disturbances
  - CMEs: Long-duration & strong IMF Bs. *Source:* solar eruptions
  - CIRs & HSS: Long-lived (up to ten days) intervals of high  $V_{\text{sw}}$  & fluctuating Bs. Typical IMF is oblique with small  $\pm B_z$ . *Source:* Coronal Holes
  - Sheath regions: shocks, high  $P_{\text{dyn}}$ , high  $V_{\text{sw}}$ , compressed IMF Bs *Source:* propagation of solar ejecta through heliosphere

# Geoeffectiveness: Modifying Factors

## Modifiers

- **Solar Wind Density**
  - Correlated with plasma sheet density (ring current source) [c.f., *Borovsky et al.*, 1998]
  - Effects strength of ring current & magnetic storm
- **Low Alfvén Mach no.** (high  $B_s$ , low  $N_{sw}$ )
  - Associated with saturation of the polar cap potential [*Ridley* 2005, 2007; *Kivelson and Ridley*, 2008]
  - Modifies magnetospheric response to extreme drivers
- **Northward IMF**
  - Efficient capture of solar wind plasma - can produce cold dense plasma sheet [c.f., *Li et al.*, 2009]
  - If delivered to inner region by subsequent IMF  $B_s$ - amplifies ring current & storm intensity [*Thomsen et al.*, 2003]
  - Is this a factor in complex ICME ejecta?

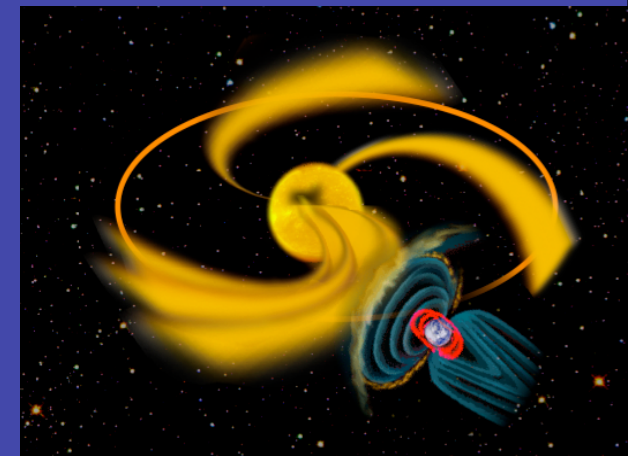
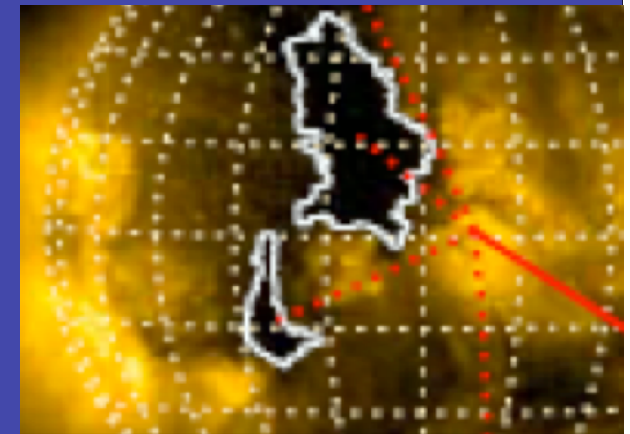
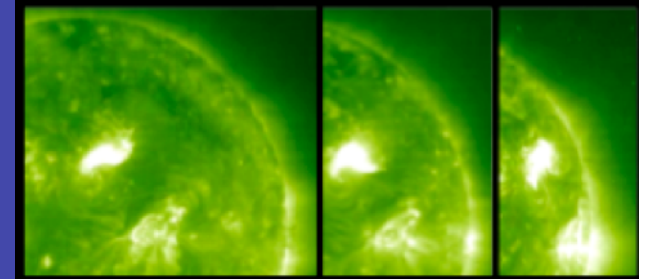
# Geoeffectiveness: Solar complexity

## Super Active Regions (multiple eruptions)

- First CME clears path for rapid transit of subsequent CMEs [c.f., *Manchester et al.*, 2008]
- Previous CME still attached to AR provides scatter free pathway for SEP transit (CME Superhighway) [*Cane et al.*, 2005]
- Earlier eruptions precondition Geospace as new CMEs arrive

## Open magnetic flux (Low latitude coronal holes)

- CHs deflect CMEs either toward or away from the Earth - deflected CME in 20 Nov 2003 superstorm closer to sun-Earth line [*Gopalswamy et al.*, 2009]
- CH-AR-Current Sheet (CHARCS) structures: intense storms associated with ARs close to the streamer belt and to growing low-latitude CHs [*Gonzalez et al.*, 1996].
- Distribution of low-latitude CHs controls geospace energy input during the declining phase of the SC. Can differ from cycle to cycle [*Gibson et al.*, 2009]



# Geoeffectiveness: Solar complexity

## CME-CME interactions

- Produce more efficient acceleration and stronger SEP events [*Gopalswamy et al.*, 2003]
- Produce complex ICMEs that intensify storms [*Farrugia et al.*, 2006]

Highly inclined CMEs with strong axial Bs - extremely geo-effective type of CME. Difficult to predict [*Gopalswamy et al.*, 2005]



# References

# References

- Borovsky, J. E., M. F. Thomsen, and R. C. Elphic, The driving of the plasma sheet by the solar wind, *J. Geophys. Res.*, 1998
- Borovsky, J. E., and M. H. Denton (2006), The effect of plasmaspheric drainage plumes on solar-wind/magnetosphere coupling, *Geophys. Res. Lett.*, 33, L20101, doi:10.1029/2006GL026519.
- Borovsky, J. E., M. Hesse, J. Birn, and M. M. Kuznetsova (2008), What determines the reconnection rate at the dayside magnetosphere?, *J. Geophys. Res.*, 113, A07210, doi:10.1029/2007JA012645.
- Cane, et al., Why did the January 20 2005 GLE Have Such a Rapid Onset?, *Eos Trans. AGU*, 86(52), Fall Meet. Suppl., Abstract SH21A-05
- Chen, S.-H., and T. E. Moore (2006), Magnetospheric convection and thermal ions in the dayside outer magnetosphere, *J. Geophys. Res.*, 111, A03215, doi:10.1029/2005JA011084.
- Crooker, N.U., Dayside merging and cusp geometry, *J. Geophys. Res.*, 84, 951, 1979.
- Dungey, J. W., Interplanetary magnetic field and the auroral zone, *Phys. Rev. Lett.*, Vol. 6, No. 2, 47-48, 1961
- Emslie, A. G., et al. (2004), Energy partition in two solar flare/CME events, *J. Geophys. Res.*, 109, A10104, doi:10.1029/2004JA010571.
- Farrugia, C. J., V. K. Jordanova, M. F. Thomsen, G. Lu, S. W. H. Cowley, and K. W. Ogilvie (2006), A two-ejecta event associated with a two-step geomagnetic storm, *J. Geophys. Res.*, 111, A11104, doi:10.1029/2006JA011893.
- Gibson, S. E., J. U. Kozyra, G. de Toma, B. A. Emery, T. Onsager, and B. J. Thompson (2009), If the Sun is so quiet, why is the Earth ringing? A comparison of two solar minimum intervals, *J. Geophys. Res.*, 114, A09105, doi:10.1029/2009JA014342.
- Gonzalez, W.D., B.T. Tsurutani, A.L.C. Gonzalez, E.J. Smith, F. Tang and S.-I. Akasofu, Solar wind-magnetosphere coupling during intense magnetic storms (1978-1979), *J. Geophys. Res.*, 94, 8835, 1989.
- Gonzalez, W. D., J. A. Joselyn, Y. Kamide, H.W. Kroehl, G. Rostoker, B. T. Tsurutani, and V. M. Vasylunas, What is a geomagnetic storm?, *J. Geophys. Res.*, 99, A4, 5771-5792, 1994.
- Gonzalez, W. D., B. T. Tsurutani, P. S. McIntosh, A. L. Clua de Gonzalez, Coronal Hole - Active Region - Current Sheet (CHARCS) association with intense interplanetary and geomagnetic activity, *Geophys. Res. Lett.*, Vol. 23, No. 19, 2577-2580, 1996.
- Gopalswamy, N., S. Yashiro, G. Michalek, M. L. Kaiser, R. A. Howard, R. Leske, T. von Roseninge and D. V. Reames, Effect of CME Interactions on the Production of Solar Energetic Particles, *Solar wind ten: Proceedings of the Tenth International Solar Wind Conference*, edited by M. Velli, R. Bruno, and F. Malara, American Institute of Physics, 2003
- Gopalswamy, N., S. Yashiro, G. Michalek, H. Xie, R. P. Lepping, and R. A. Howard (2005), Solar source of the largest geomagnetic storm of cycle 23, *Geophys. Res. Lett.*, 32, L12S09, doi:10.1029/2004GL021639.
- Gopalswamy, N., P. Ma'kela', H. Xie, S. Akiyama, and S. Yashiro (2009), CME interactions with coronal holes and their interplanetary consequences, *J. Geophys. Res.*, 114, A00A22, doi:10.1029/2008JA013686

# References

- Greenspan, M.E., and D. C. Hamilton, Relative contributions of H<sup>+</sup> and O<sup>+</sup> to the ring current energy near magnetic storm maximum, *J. Geophys. Res.*, Vol. 107, No. A4, 1043, 10.1029/2001JA000155, 2002
- Hecht, J. H., et al. (2008), Satellite and ground-based observations of auroral energy deposition and the effects on thermospheric composition during large geomagnetic storms: 1. Great geomagnetic storm of 20 November 2003, *J. Geophys. Res.*, 113, A01310, doi:10.1029/2007JA012365
- Huang, C. Y., and W. J. Burke (2004), Transient sheets of field-aligned current observed by DMSP during the main phase of a magnetic superstorm, *J. Geophys. Res.*, 109, A06303, doi:10.1029/2003JA010067.
- Ieda, A., S. Machida, T. Mukai, Y. Saito, T. Yamamoto, A. Nishida, T. Terasawa, and S. Kokubun, Statistical analysis of the plasmoid evolution with Geotail observations, *J. Geophys. Res.*, 103, 4453–4465, 1998.
- Kivelson, M. G., and A. J. Ridley (2008), Saturation of the polar cap potential: Inference from Alfvén wing arguments, *J. Geophys. Res.*, 113, A05214, doi:10.1029/2007JA012302
- Laitinen, T. V., M. Palmroth, T. I. Pulkkinen, P. Janhunen, and H. E. J. Koskinen (2007), Continuous reconnection line and pressure-dependent energy conversion on the magnetopause in a global MHD model, *J. Geophys. Res.*, 112, A11201, doi:10.1029/2007JA012352.
- Lavraud, B., M. H. Denton, M. F. Thomsen, J. E. Borovsky, and R. H.W. Friedel, Superposed epoch analysis of dense plasma access to geosynchronous orbit, *Annales Geophysicae*, 23, 2519–2529, 2005
- Lavraud, B., M. F. Thomsen, B. Lefebvre, S. J. Schwartz, K. Seki, T. D. Phan, Y. L. Wang, A. Fazakerley, H. Re`me, and A. Balogh (2006), Evidence for newly closed magnetosheath field lines at the dayside magnetopause under northward IMF, *J. Geophys. Res.*, 111, A05211, doi:10.1029/2005JA011266.
- Lavraud, B., M. F. Thomsen, S. Wing, M. Fujimoto, M. H. Denton, J. E. Borovsky, A. Aasnes, K. Seki, and J. M. Weygand, Observation of two distinct cold, dense ion populations at geosynchronous orbit: local time asymmetry, solar wind dependence and origin, *Ann. Geophys.*, 24, 3451–3465, 2006
- Li, W., J. Raeder, J. Dorelli, M. Øieroset, and T. D. Phan (2005), Plasma sheet formation during long period of northward IMF, *Geophys. Res. Lett.*, 32, L12S08, doi:10.1029/2004GL021524.
- Li, W., J. Raeder, M. Øieroset, and T. D. Phan (2009), Cold dense magnetopause boundary layer under northward IMF: Results from THEMIS and MHD simulations, *J. Geophys. Res.*, 114, A00C15, doi:10.1029/2008JA013497.
- Lotko, W., The magnetosphere–ionosphere system from the perspective of plasma circulation: A tutorial, *Journal of Atmospheric and Solar-Terrestrial Physics* 69 (2007) 191–211
- Luhmann, J. G., R. J. Walker, C. T. Russell, N. U. Crooker, J. R. Spreiter, and S. S. Stahara, Patterns of potential magnetic field merging sites on the dayside magnetopause, *J. Geophys. Res.*, 89, A3, 1739-1742, 1984.

# References

- Manchester IV, W.B., A. Vourlidas, G. Toth, N. Lugaz, I.I. Roussev, I. V. Sokolov, T. I. Gombosi, D. L. De Zeeuw, and M. Opher, THREE-DIMENSIONAL MHD SIMULATION OF THE 2003 OCTOBER 28 CORONAL MASS EJECTION: COMPARISON WITH LASCO CORONAGRAPH OBSERVATIONS, *The Astrophysical Journal*, 684:1448Y1460, 2008.
- Maynard, N. C., et al. (2002), Predictions of magnetosheath merging between IMF field lines of opposite polarity, *J. Geophys. Res.*, 107(A12),1456, doi:10.1029/2002JA009289.
- Maynard, N. C., et al. (2003), Polar, Cluster and SuperDARN evidence for high-latitude merging during southward IMF: Temporal/spatial evolution, *Ann. Geophys.*, 21, 2233–2258.
- Mewaldt, R. A., C. M. S. Cohen, A. W. Labrador, R. A. Leske, G. M. Mason, M. I. Desai, M. D. Looper, J. E. Mazur, R. S. Selesnick, and D. K. Haggerty (2005), Proton, helium, and electron spectra during the large solar particle events of October–November 2003, *J. Geophys. Res.*, 110, A09S18, doi:10.1029/2005JA011038.
- Mlynczak, M. G., et al. (2005), Energy transport in the thermosphere during the solar storms of April 2002, *J. Geophys. Res.*, 110, A12S25, doi:10.1029/2005JA011141.
- Mlynczak, M. G., F. J. Martin-Torres, and J. M. Russell III (2007), Correction to “Energy transport in the thermosphere during the solar storms of April 2002,” *J. Geophys. Res.*, 112, A02303, doi:10.1029/2006JA012008.
- Moore, T. E., and J. L. Horwitz (2007), Stellar ablation of planetary atmospheres, *Rev. Geophys.*, 45, RG3002, doi:10.1029/2005RG000194.
- Moore, T. E., W. K. Peterson, C. T. Russell, M.O. Chandler, M.R. Collier, H.L. Collin, P. D. Craven, R. Fitzenreiter, B. L. Giles, and C. J. Pollock, Ionospheric mass ejection in response to a CME, *Geophys Res. Lett.*, Vol., 26, No. 15, 2339-2342, 1999.
- Nose, M., S. Taguchi, K. Hosokawa, S. P. Christon, R. W. McEntire, T. E. Moore, and M. R. Collier (2005), Overwhelming O<sup>+</sup> contribution to the plasma sheet energy density during the October 2003 superstorm: Geotail/EPIC and IMAGE/LENA observations, *J. Geophys. Res.*, 110, A09S24, doi:10.1029/2004JA010930.
- Nowada, M., J.-H. Shue, C. T. Russell, Effects of dipole tilt angle on geomagnetic activity, *Planet. Space Sci.*, 57 (2009) 1254-1259.
- Ogino, T., R. J. Walker, M. Ashour-Abdalla, J. M. Dawson, An MHD simulation of the effects of the interplanetary magnetic field By component on the interaction of the solar wind with the Earth’s magnetosphere during southward interplanetary magnetic field, *J. Geophys. Res.*, 91, A9, 10029-10045, 1986.
- Øieroset, M., J. Raeder, T. D. Phan, S. Wing, J. P. McFadden, W. Li, M. Fujimoto, H. Re`me, and A. Balogh (2005), Global cooling and densification of the plasma sheet during an extended period of purely northward IMF on October 22–24, 2003, *Geophys. Res. Lett.*, 32, L12S07, doi:10.1029/2004GL021523
- Øieroset, M., T. D. Phan, V. Angelopoulos, J. P. Eastwood, J. McFadden, D. Larson, C. W. Carlson, K.-H. Glassmeier, M. Fujimoto, and J. Raeder (2008), THEMIS multi-spacecraft observations of magnetosheath plasma penetration deep into the dayside lowlatitude magnetosphere for northward and strong By IMF, *Geophys. Res. Lett.*, 35, L17S11, doi:10.1029/2008GL033661.

# References

- Palmroth, M.. Solar wind - magnetosphere interaction as determined by observations and a global MHD simulation, PhD thesis, 2003
- Palmroth, M., P. Janhunen, and T. I. Pulkkinen (2006), Hysteresis in solar wind power input to the magnetosphere, *Geophys. Res. Lett.*, 33, L03107, doi:10.1029/2005GL025188.
- Park, K. S., T. Ogino, and R. J. Walker (2006), On the importance of antiparallel reconnection when the dipole tilt and IMF By are nonzero, *J. Geophys. Res.*, 111, A05202, doi:10.1029/2004JA010972.
- Pollock, C.J., T.E.Moore, D.Gurnett, J.A.Slavin, J.H.Waite,Jr., Observations of electric and magnetic field signatures in association with upwelling ion events, *Eos* 69(44), p.1396, 1988.
- Pulkkinen, T. I., M. Palmroth, E. I. Tanskanen, P. Janhunen, H. E. J. Koskinen, and T. V. Laitinen (2006), New interpretation of magnetospheric energy circulation, *Geophys. Res. Lett.*, 33, L07101, doi:10.1029/2005GL025457.
- Pulkkinen, T.I., M. Palmroth, E.I. Tanskanen, N.Yu.. Ganushkina, M.A. Shukhtina, N. P. Dmitrieva,Solar wind - magnetosphere coupling: A review of recent results, *J. Atmos. Sol. Terr. Phys.*, 69 (2007) 256-264.
- Pulkkinen, T. I., M.Palmroth, T.Laitinen, Energy as a tracer of magnetospheric processes: GUMICS-4 global MHD results and observations compared, *J. Atmos. Sol Terr. Phys.*, 70 (2008) 687.707.
- Reiff, P. H., Sunward convection in both polar caps, *J. Geophys. Res.*, 87, A8, 5976-5980, 1982
- Ridley, A. J. (2005), A new formulation for the ionospheric cross polar cap potential including saturation effects, *Ann. Geophys.*, 23, 3533.
- Ridley, A. J. (2007), Alfvén wings at Earth's magnetosphere under strong interplanetary magnetic field, *Ann. Geophys.*, 25, 533.
- Robinson, R. M., S. B. Mende, R. R. Vondrak, J. U. Kozyra, and A. F. Nagy, Radar and photometric measurements of an intense type A red aurora, *J. Geophys. Res.*, 90, 457-466, 1985.
- Russell, C. T., Y.L. Wang, and J. Raeder, Possible dipole tilt dependence of dayside magnetopause reconnection, *Geophys. Res. Lett.* Vol., 30, No. 18, 1937, doi:10.1029/2003GL017725, 2003.
- Sandholt, P. E., C.J. Farrugia, S. W. H. Cowley, and M. Lester, Dayside auroral bifurcation sequence during By-dominated interplanetary magnetic field: relationship with merging and lobe convection cells, *J. Geophys. Res.*, 106, A8, 15429-15444, 2001.
- Schunk, R. W., H. G. Demars, J. J. Sojka, Propagating polar wind jets, *Journal of Atmospheric and Solar-Terrestrial Physics* 67 (2005) 357–364
- Shiokawa K., C.-I. Meng, G. D. Reeves, F. J. Rich, and K. Yumoto, A multievent study of broadband electrons observed by the DMSP satellites and their relation to red aurora observed at midlatitude stations, *J. Geophys. Res.*, 102, A7, 14237-14253, 1997.
- Shue, J.-H., 1993. Dependence of the ionospheric convection pattern on the conductivity and the southward IMF. Ph.D. Thesis, University of Alaska, Fairbanks.
- Shue, J.-H.. P. T. Newell, K.Liou, C.-I. Meng, Y. Kamide, and R. P. Lepping, Two-component auroras, *Geophys. Res. Lett.*, Vol. 29, No. 10, 10.1029/2002GL014657, 2002.

# References

- Smith, M. F., and M. Lockwood, Earth's magnetospheric usps,R ev. Geophys., 34, 233-260, 1996.
- Sojka, J.J. and L. Zhu, Multiple arcs: Evidence for an active ionospheric role in the M-I coupling, Advances in Space Research 38 (2006) 1702–1706
- Strangeway, R. J., R. E. Ergun, Y.-J. Su, C. W. Carlson, and R. C. Elphic (2005), Factors controlling ionospheric outflows as observed at intermediate altitudes, J. Geophys. Res., 110, A03221, doi:10.1029/2004JA010829
- Tanaka, T., Magnetosphere-Ionosphere convection as a compound system, Space Sci. Rev., (2007) 133: 1-72.
- Thomsen, M. F., J. E. Borovsky, R. M. Skoug, and C. W. Smith, Delivery of cold, dense plasma sheet material into the near-Earth region, J. Geophys. Res., 108(A4), 1151, doi:10.1029/2002JA009544, 2003.
- Vallance Jones, A., Historical review of great auroras, Can J. Phys., 70, 479, 1992
- Watanabe, M., K. Kabin, G. J. Sofko, R. Rankin, T. I. Gombosi, A. J. Ridley, and C. R. Clauer (2005), Internal reconnection for northward interplanetary magnetic field, J. Geophys. Res., 110, A06210, doi:10.1029/2004JA010832.
- Weiss, L. A., P. H. Reiff, E. J. Weber, H. C. Carlson, M. Lockwood, and W. K. Peterson, Flow-aligned jets in the magnetospheric cusp: Results from the Geospace Environment Modeling Pilot program, J. Geophys. Res., 100, A5, 7649-7659, 1995.
- Wing, S., P. T. Newell and J. M. Ruohoniemi, Double cusp: Model prediction and observational verification, J. Geophys. Res., 106, A11, 25571-25593, 2001
- Winglee, R.M., Chua, D., Brittnacher, M., Parks, G.K., Lu, G.,2002. Global impact of ionospheric outflows on the dynamics of the magnetosphere and cross-polar cap potential. Journal of Geophysical Research 107 (A9), 1237.
- Zhou, X.-W. and C.T. Russell, The location of the high-latitude polar cusp and the shape of the surrounding magnetopause, J. Geophys. Res., 102, A1, 105-110, 1997.
- Zhu, L., J.J. Sojka, R.W. Schunk, Active ionospheric role in small-scale aurora structuring, Journal of Atmospheric and Solar-Terrestrial Physics 67 (2005) 687–700